Supplementary Information

Efficient templated synthesis of pillar[6]arenes by *in situ* generated Lewis adducts

Alexia Dussart[1], Sébastien Lengelé[1], Ivan Jabin[1,*], Roy Lavendomme[1,2,*]

[1] Laboratoire de Chimie Organique, Université libre de Bruxelles (ULB), Avenue F. D. Roosevelt 50, CP160/06, B-1050 Brussels, Belgium
[2] Laboratoire de Résonance Magnétique Nucléaire Haute Résolution, Université libre de Bruxelles (ULB), Avenue F. D. Roosevelt 50, CP160/08, B-1050 Brussels, Belgium

Table of Contents

1. Instrumentation and Methods

Commercial $CHCl_3$ and CH_2Cl_2 contained amylene as stabilizer and was used without further purification. Anhydrous CH_2Cl_2 was distilled over CaH_2. All other reactants and reagents were obtained from commercial sources and used without further purification. Column chromatography was performed on silica gel 60 (particle size 40–63 µm).

NMR analyses were performed using a Bruker Avance DPX 300 operating at 7.0 T (300 MHz for ^1H) equipped with a 5 mm probe with z-PFG for double resonance experiments, JEOL JNM-ECZ400R/S3 operating at 9.4 T (400 MHz for ^1H) equipped with a double resonance ROYALTM probe, or JNM-ECZ600R/S3 spectrometer operating at 14.1 T (600 MHz for ^1H) equipped with a double resonance ROYALTM probe. ^1H and ^{13}C spectra were referenced with respect to the residual signal of the solvent (^1H: $CHCl_3$ at 7.26 ppm, DMSO-d_5 at 2.50 ppm).

Infrared spectra (IR) were recorded on a FTIR spectrometer model Shimadzu IRSpirit equipped with diamond ATR module (QATR-S).

2. Synthesis and spectral characterization

2.1. Dodecaethoxypillar[6]arene **P[6]OEt** (1g)

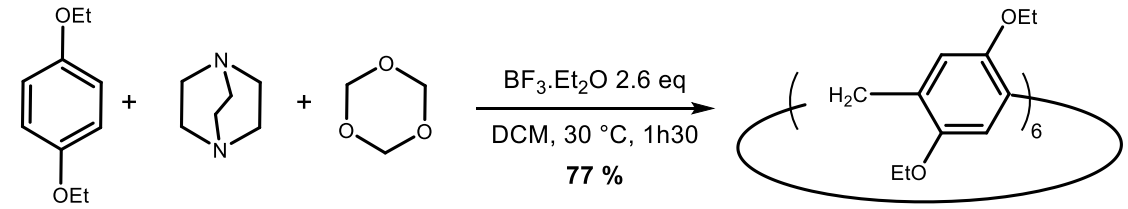

MW: 166.22 MW: 112.18 MW: 90.08 MW: 1069.39

P[6]OEt

In a round bottomed flask, to a mixture of 1,4-diethoxybenzene (1.00 g, 6.02 mmol), 1,3,5-trioxane (0.362 g, 4.02 mmol, 0.67 eq.), and 1,4-diazabicyclo[2.2.2]octane (0.169 g, 1.51 mmol, 0.25 eq.) in dichloromethane (30 mL, see Note 1) stirred at r.t. (23 °C) was added $BF_3{\cdot}Et_2O$ (1.9 mL, d = 1.15 g/L, 2.19 g, 15.4 mmol, 2.56 eq.). The mixture was then stirred at 30 °C for 1h30 (Note 2) and the color evolved from white to green (after 30 min.) to blue to black (see Fig. S1 and S2). Quickly after the mixture turned black, the reaction was quenched with methanol (1/5 V = 6 mL). The resulting beige suspension was stirred at r.t. for 24 hours (Note 3).

The mixture was filtered and washed with dichloromethane (5 mL). The filtrate was washed with HCl 1 M (20 mL) twice (Note 4) and the combined aqueous layers were washed with dichloromethane (25 mL). The combined organic layers were evaporated under reduced pressure to afford a dark green residue (1.85 g).

The product was purified by flash column chromatography on silica gel with solid deposit adsorbed on celite (eluent: dichloromethane/acetone, 1:0 → 49:1), affording **P[5]OEt** in the first fraction (23.2 mg, 0.0260 mmol, yield: 2.2%) and **P[6]OEt** in the second fraction (822 mg, 0.769 mmol, yield: 77%) as a slightly orange tinted white solid. Spectral data is in accordance with the literature.[S1]

Notes: (1) The reaction can be done in chloroform with the same conditions, work-up and purification method, except shorter reaction time in the range 1h00–1h30 for complete substrate consumption, affording **P[6]OEt** with a yield of 70%. Using $CHCl_3$ typically leads to smaller amounts of **P[5]OEt** (0–2%).

(2) The reaction time may vary but completion was always observed between 1h30 and 2h00. The completion of the reaction can be observed with the evolution of the color: it turns black once the monomer is completely consumed. The conversion of the monomer can be monitored by TLC, R_f (SiO_2, cyclohexane/ethyl acetate 8:2) of the monomer: 0.8.

(3) Lengthy reaction quenching with methanol is necessary to break the Lewis adduct template. Quenching time requires at least overnight stirring and was performed over 24h to be safe.

(4) Although it was not performed in this case, it was later found that a supplementary wash with neutral H_2O after acidic washes could be beneficial to remove traces of acid that may generate polymers.

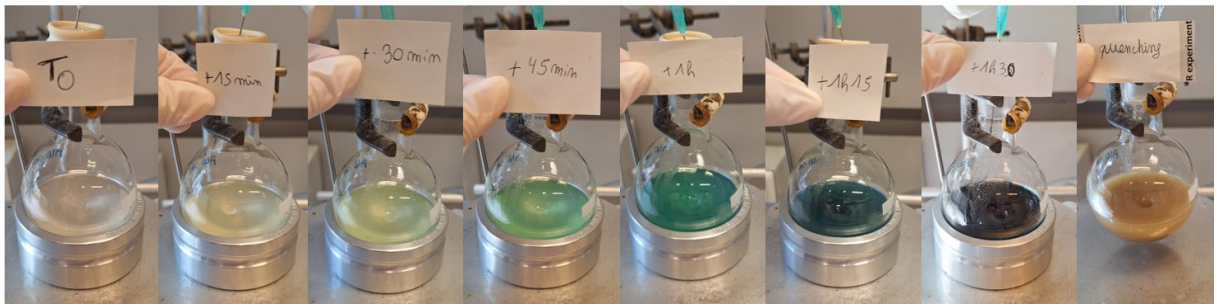

Figure S1. Color evolution of the reaction for the 1 g scale synthesis of **P[6]OEt** in DCM, 30 °C (from left to right: 0 min., 15 min., 30 min., 45 min., 1h00, 1h15, 1h30, quenching with MeOH).

Figure S2. Color evolution of the reaction for the 1 g scale synthesis of **P[6]OEt** in DCM, 30 °C (from left to right: 15 min., 30 min., 45 min., 1h00, 1h15, 1h30).

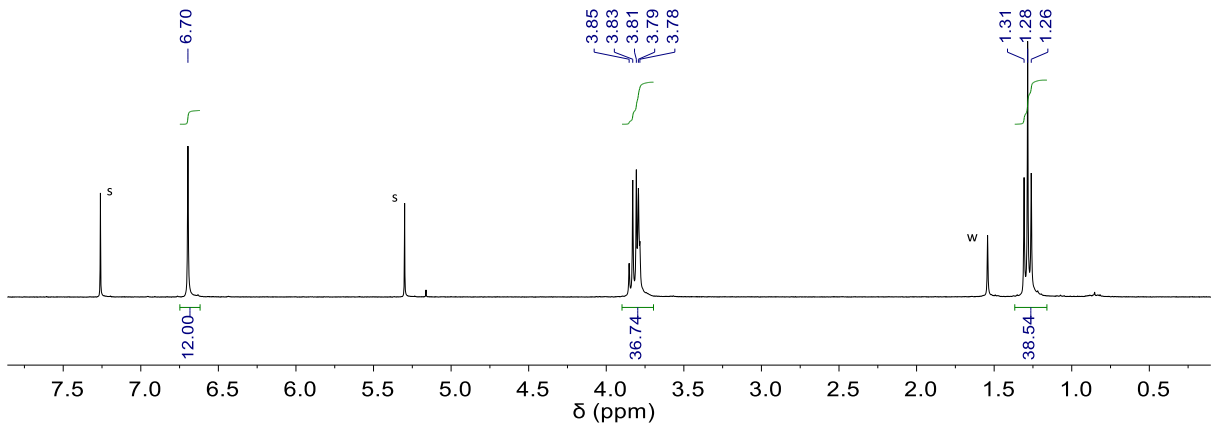

Figure S3. ^{1}H NMR spectrum (300 MHz, $CDCl_3$, 298 K) of **P[6]OEt**. s: solvents, w: water.

2.2. Dodecaethoxypillar[6]arene **P[6]OEt** (30 g)

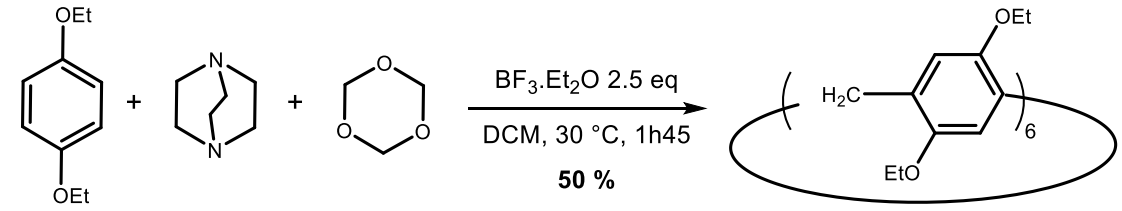

MW: 166.22 MW: 112.18 MW: 90.08 MW: 1069.39

P[6]OEt

In a round bottomed flask, to a mixture of 1,4-diethoxybenzene (30.0 g, 0.180 mol) and 1,3,5-trioxane (10.8 g, 0.120 mol, 0.67 eq.) and 1,4-diazabicyclo[2.2.2]octane (5.03 g, 0.0448 mol, 0.25 eq.) in dichloromethane (900 mL) stirred at 30 °C, was added $BF_3{\cdot}Et_2O$ (55.5 mL, d = 1.15 g/L, 63.8 g, 0.450 mol, 2.5 eq.). The mixture was stirred at 30 °C for 1h45 (Note 1) and the color evolved from white to green (after 30 min.) to blue to black (see Fig. S4 and S5). Quickly after the mixture turned black, the reaction was quenched with methanol (1/5 V = 180 mL). The resulting black suspension (see Fig. S6) was stirred at r.t. for 21 hours (Note 2).

The mixture was filtered on a celite pad and washed with dichloromethane until the washing filtrate appeared colorless (see Fig. S7a). The dark brown filtrate was evaporated under reduced pressure until the volume was estimated to be 1 L. The filtrate was washed with $HCl_{aq.}$ 1 M (2 x 400 mL) then with $Na_2CO_{3\ aq.}$ 1 M (2 x 400 mL) (see Note 3 and Fig. S7b). The dark orange organic layer was evaporated under reduced pressure then redissolved in DCM (200 mL) (Note 4). The mixture was filtered again on a celite pad, which was rinsed with dichloromethane until the washing filtrate appeared colorless. The filtrate was evaporated under reduced pressure (27.49 g).

The orange residue was dissolved in dichloromethane (100 mL). Acetone (1.5 V = 150 mL) was added while gently stirring then methanol was added (0.5 V = 50 mL) (see Fig. S8). The mixture was left to rest overnight at r.t. to obtain larger grains (Note 5). The precipitate was collected by filtration through a Büchner funnel and washed with acetone until the washing filtrate appeared colorless. The light orange solid was dried under high vacuum to afford **P[6]OEt** (16.4 g, 90% purity*, 13.8 mmol, 46 % yield corrected for purity; 10% of acetone* corresponding to 2 equiv. presumably stuck in the cavity). A second fraction of product was collected from the filtrate: the filtrate was evaporated under reduced pressure, the residue (6.95 g) was dissolved in dichloromethane (30 mL). Acetone (4 V = 120 mL) was added while gently stirring then methanol was added (1/6 V = 5 mL). The mixture was left to rest overnight at r.t. to obtain larger grains. The precipitate was filtered through a Büchner funnel and washed with acetone until the washing filtrate appeared colorless. The orange solid was dried under high vacuum to afford a second fraction of **P[6]OEt** (1.73 g, 80 % purity*, 1.29 mmol, 4 % yield corrected for purity; 8 % of acetone*).

Total mass of **P[6]OEt** obtained over the two fractions: 16.1 g (weight fraction of **P[6]OEt** without solvents), 15.1 mmol, yield 50%.

* Measured by quantitative ^1H NMR spectroscopy ($CDCl_3$, 298 K, 300 MHz) with 1,3,5-tribromobenzene and 4-nitrotoluene as internal standards.

Notes: (1) The reaction time may vary but completion was always observed between 1h30 and 2h00. The completion of the reaction can be observed with the evolution of the color: it turns black once the monomer is completely consumed. The conversion of the monomer can be monitored by TLC, R_f (SiO_2, cyclohexane/ethyl acetate 8:2) of the monomer: 0.8. Reactions quenched before the complete consumption of the monomer will lead to colorless to very light brown mixtures (Figure S6a). Reactions quenched right after consumption of the monomer will lead to brown-dark brown mixtures (Figure S6b). Continued reaction beyond the consumption of the monomer will lead to the slow increase of polymeric material, which may render subsequent purification more difficult, and black colored mixture upon quenching (Figure S6c).

(2) Lengthy reaction quenching with methanol is necessary to break the Lewis adduct template. Quenching time requires at least overnight stirring and was performed over 21h to be safe.

(3) Acidic aqueous washes allow for the extraction of DABCO but remaining acid traces led to small amounts of polymeric films upon evaporation (perhaps paraformaldehyde films from trioxane polymerization) that rendered the purification more difficult. Therefore, subsequent neutral or basic aqueous washes were necessary. Neutral washes led to darker residues and a more challenging isolation of colorless product whereas basic washes led to orange colored residue from which colorless product is easier to isolate. Basic washes (both Na_2CO_3 aq. and NH_4OH were tested) lead to opaque organic layers, possibly, limiting the solubility of **P[6]OEt**.

(4) Evaporation of solvent and redissolution is an important step as some impurities are initially soluble in the organic layer after aqueous washes but do not redissolve after evaporation, thus allowing their removal by filtration.

(5) Precipitation with only acetone led to high purity of **P[6]OEt** but the filtration proved difficult due to the very fine powder blocking filters. Amongst the purification techniques tested, evaporation from a CH_2Cl_2/acetonitrile solution led to large block crystals of **P[6]OEt** but other oligomers tended to precipitate with the product in these conditions.

Figure S4. Color evolution of the reaction for the 30 g scale synthesis of **P[6]OEt** in DCM, 30 °C (0 min., 15 min., 30 min., 45 min., 1h00, 1h15, 1h30, 1h45, quenching with MeOH).

Figure S5. Color evolution of the reaction for the 30 g scale synthesis of **P[6]OEt** in DCM, 30 °C (15 min., 30 min., 45 min., 1h00, 1h15, 1h30, 1h45, quenching with MeOH).

Figure S6. a) reaction quenched too early, b) reaction quenched in time, c) reaction quenched too late.

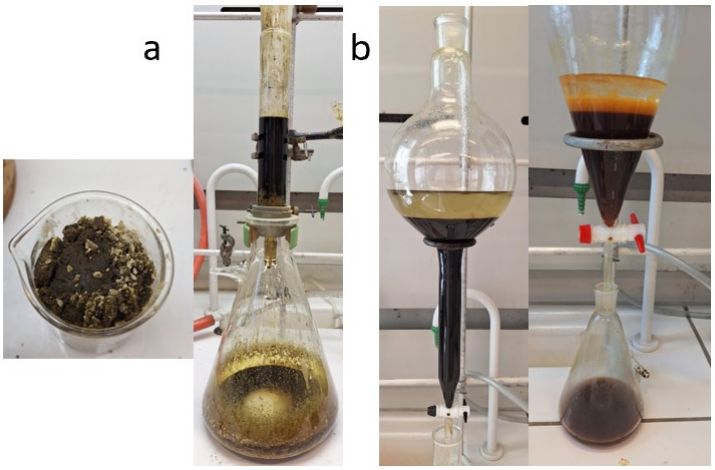

Figure S7. a) Filtration of the crude on a celite pad after quenching with MeOH for 21h then washing with DCM, b) Extraction of the filtrate with $HCl_{aq.}$ 1 M (left) then with $Na_2CO_{3\ aq.}$ 1 M (right).

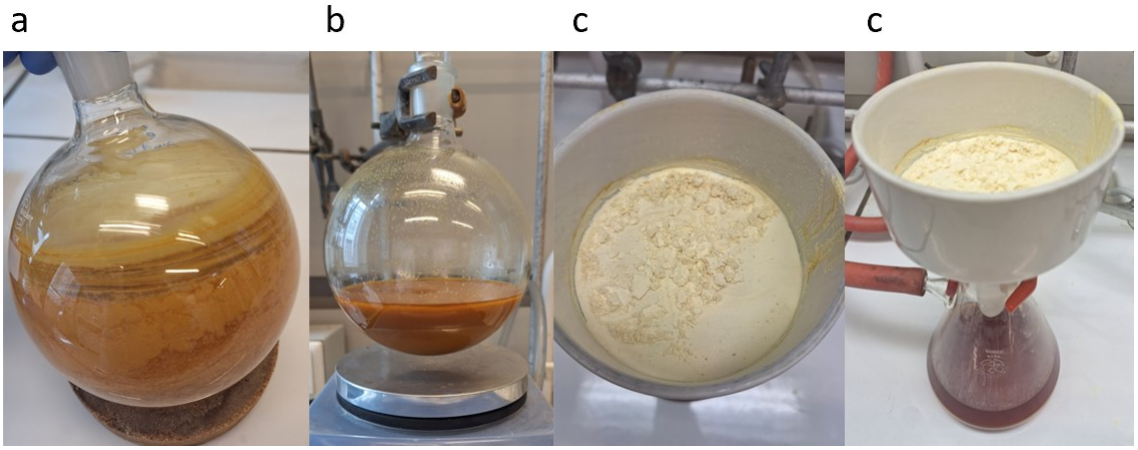

Figure S8. a) Organic layer containing **P[6]OEt** evaporated under reduced pressure after extraction with HCl 1 M then with Na_2CO_3, b) precipitation of **P[6]OEt** in DCM/acetone/MeOH 1/1.5/0.5 v/v/v, c) Filtration through a Büchner funnel, washing with acetone, obtaining **P[6]OEt** as a light orange solid.

2.3. Dodecamethoxypillar[6]arene **P[6]OMe**

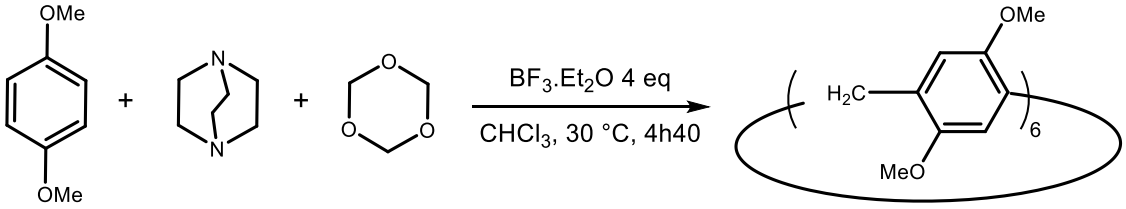

MW: 138.17 MW: 112.18 MW: 90.08 MW: 901.06

P[6]OMe

In a round bottomed flask, to a mixture of 1,4-dimethoxybenzene (1.00 g, 7.24 mmol) and 1,3,5-trioxane (0.438 g, 4.87 mmol, 0.67 eq.) and 1,4-diazabicyclo[2.2.2]octane (0.407 g, 3.63 mmol, 0.5 eq.) in chloroform (72 mL) stirred at r.t. (21 °C), was added $BF_3{\cdot}Et_2O$ (3.60 mL, d = 1.15 g/L, 4.14 g, 26.2 mmol, 4.0 eq.). The mixture was then stirred at 30 °C for 4h40 (Note 1) and the color evolved from white to green (after 3 hours) to blue to black (see Fig. S9). Quickly after the mixture turned black, acetone was added (5 V% = 3.6 mL). The mixture was filtered through cotton and washed until the washing filtrate appears colorless. The filtrate was concentrated under reduced pressure until the final volume was approximately 100 mL (Fig. S10a). Acetone was added (4V = 400 mL) (Fig. S10b) and the mixture was left to rest at 4 °C for 43h (Note 2) to obtain a suspension (Fig. S10c). The suspension was filtered and washed with acetone (45 mL) to isolate a beige solid (829 mg) (Fig. S10d). (Note 3)

Notes: (1) The reaction time may vary but completion was always observed between 2h30 and 5h30. The completion of the reaction can be observed with the evolution of the color: it turns black once the monomer is completely consumed. The conversion of the monomer can be monitored by TLC, Rf (SiO_2, dichloromethane/cyclohexane 6:4) of the monomer: 0.5.

(2) The mixture was left 43h at 4 °C for circumstantial reasons but overnight rest is expected to suffice.

(3) **P[6]OMe** exhibits peculiar solubility properties. It is initially soluble in CH_2Cl_2 or $CHCl_3$ but tends to precipitate over time in a form that does not resolubilize, even in excess solvent. Instead of letting **P[6]OMe** precipitate slowly, if the solvent is rapidly evaporated, the resulting solid is only partially soluble. ^{1}H NMR analysis of the soluble fraction corresponds to the reported spectrum of **P[6]OMe**.[S2] To verify the purity of samples exhibiting this peculiar solubility, the crude product prior to precipitation was subjected to column chromatography (SiO_2, CH_2Cl_2/acetone, 199:1) and the product fraction in solution was analyzed by ^{1}H NMR spectroscopy with presaturation of the CH_2Cl_2 signal, showing that the product corresponds indeed to **P[6]OMe** (Figure S11). Due to this peculiar solubility leaving insoluble fractions in NMR samples, the yield of **P[6]OMe** was not calculated at this step. The crude beige solid was subjected to demethylation in order to determine a yield over 2 steps (see section 2.4).

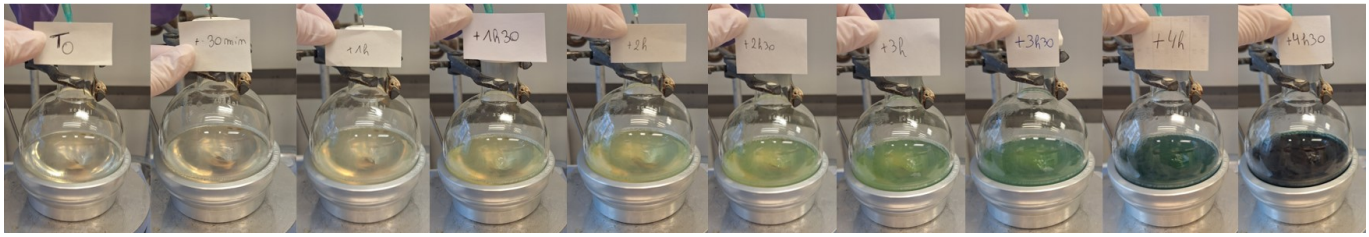

Figure S9. Color evolution of the reaction for the 1 g scale synthesis of **P[6]OMe** in chloroform, 30 °C (0 min., 30 min., 1h00, 1h30, 2h00, 2h30, 3h00, 3h30, 4h00, 4h30).

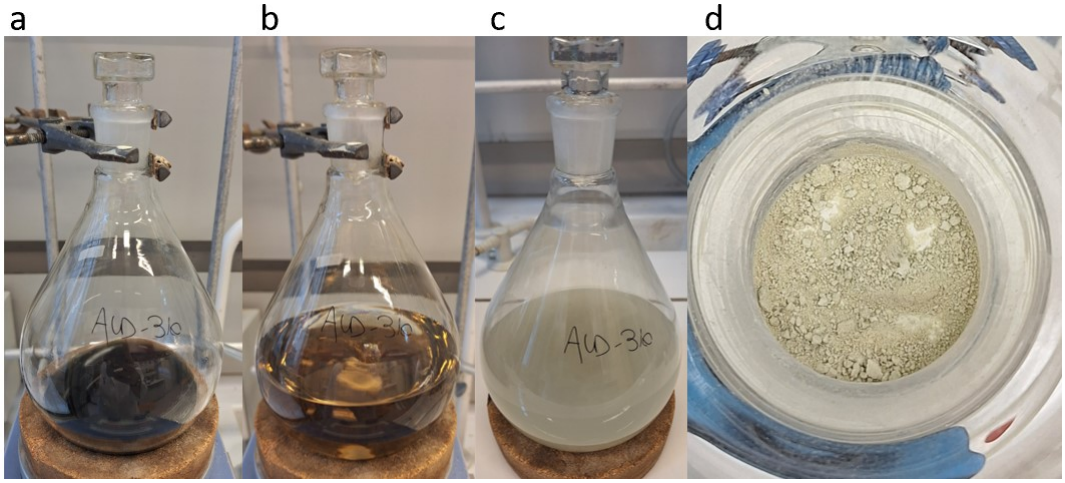

Figure S10. a) Crude of the reaction after filtration on cotton and evaporation under reduced pressure until V = 100 mL, b) Addition of acetone (4V = 400 mL), c) Suspension obtained after 43h at 4 °C, d) Filtration of the suspension to isolate a beige solid containing **P[6]OMe**.

Rf (SiO_2, DCM/acetone 99:1): 0.5

Mp: >200 °C.

IR: ν (cm^{-1}) = 685, 740, 1044, 1209, 1506.

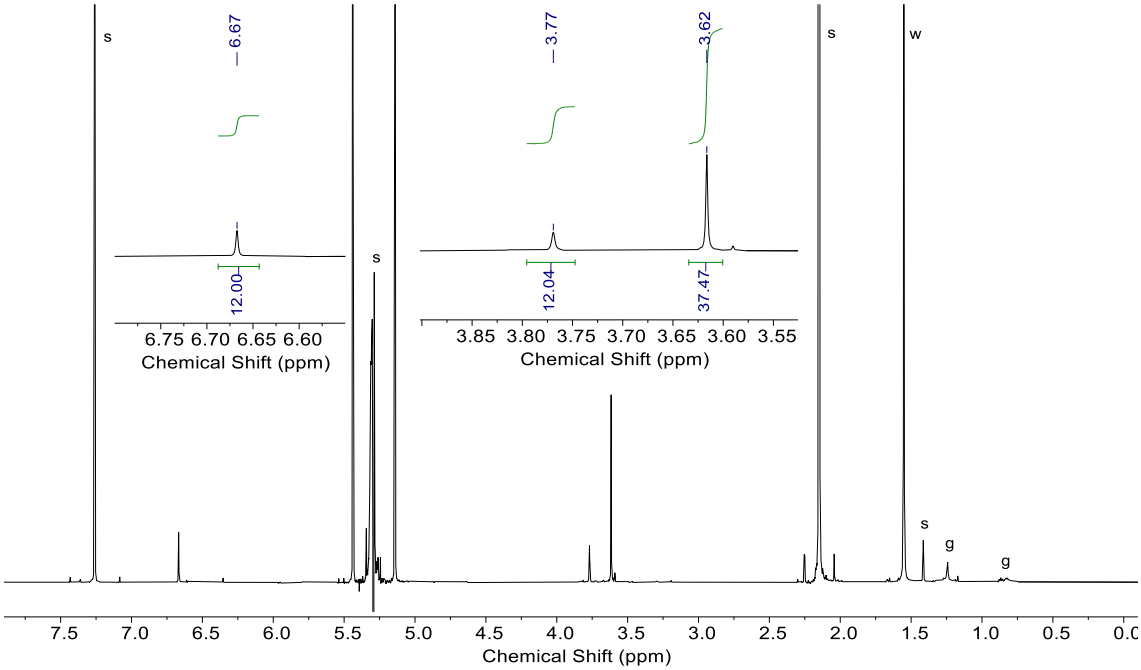

Figure S11. ^1H NMR spectrum (300 MHz, $CDCl_3$, 298 K, presaturation on CH_2Cl_2 signal) of **P[6]OMe** directly from the solution fraction after column chromatography. s: solvents, w: water, g: grease.

2.4. Dodecahydroxypillar[6]arene **P[6]OH** from crude **P[6]OMe**

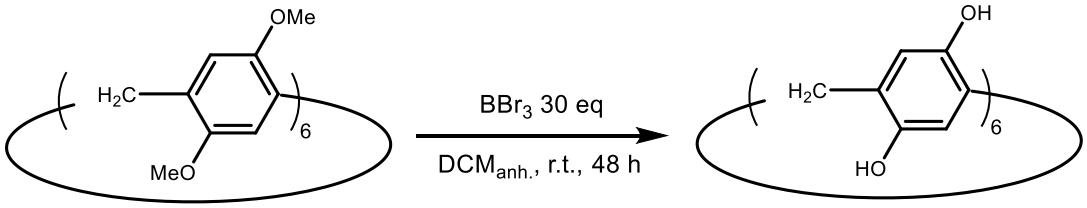

MW: 901.06
P[6]OMe

MW: 732.74
P[6]OH

In an oven-dried tube equipped with a screw cap, to a stirred suspension of **P[6]OMe** (0.829 g, 0.920 mmol) in anhydrous dichloromethane (46 mL) was added boron tribromide (2.6 mL, d = 2.65 g/mL, 6.89 g, 27.5 mmol, 30 eq.) (Fig. S12a). The mixture was stirred at r.t. (21 °C) for 48h under argon atmosphere (Fig. S12b). Methanol (1 mL) and distilled H_2O (9.2 mL) were added and the mixture was stirred for 30 min (Fig. S12c–e). The suspension was filtered and washed with distilled H_2O to afford a green solid (1.59 g) (Fig. S12f). The green solid was taken up in acetone (10 mL) and filtered through silica gel (eluent: acetone/dichloromethane 8:2) (Note 1). The organic phase was evaporated under reduced pressure then dried under high vacuum to afford a green solid (708 mg, purity* = 72 %, 0.700 mmol corrected for purity, yield over two steps from 1,4-dimethoxybenzene: 57 %) (Note 2). Spectral data are in accordance with the literature.[S3]

* Measured by quantitative ^{1}H NMR spectroscopy (DMSO-d_6, 298 K, 300 MHz) with 1,3,5-trimethoxybenzene and 1,4-diethoxybenzene as internal standards. No species other than **P[6]OH** could be observed by ^{1}H NMR.

Notes: (1) Filtration through silica gel was performed to remove green colored impurities but the solid remained overly green and no change was observed on the ^{1}H NMR analyses. A green solution in MeOH turned brown in presence of $Na_2S_2O_5$ reductant, indicating that green impurities can be chemically degraded. Green impurities are presumably not problematic for further reactions.

(2) Another procedure by precipitation with cyclohexane was later developed to remove green impurities (see section 2.5 below).

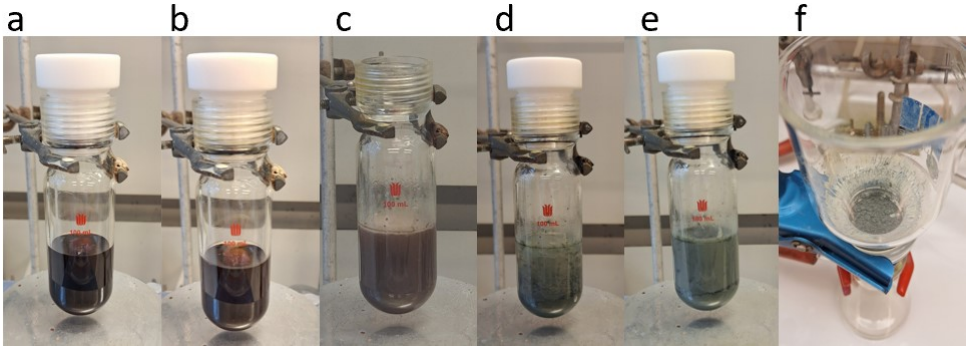

Figure S12. a) Crude of the reaction for the synthesis of **P[6]OH** after addition of boron tribromide, b) Crude of the reaction for the synthesis of **P[6]OH** after 48h, c) Addition of MeOH, d) Addition of distilled H_2O, e) Crude of the reaction for the synthesis of **P[6]OH** after 30 min of quenching, f) Filtration of the green solid.

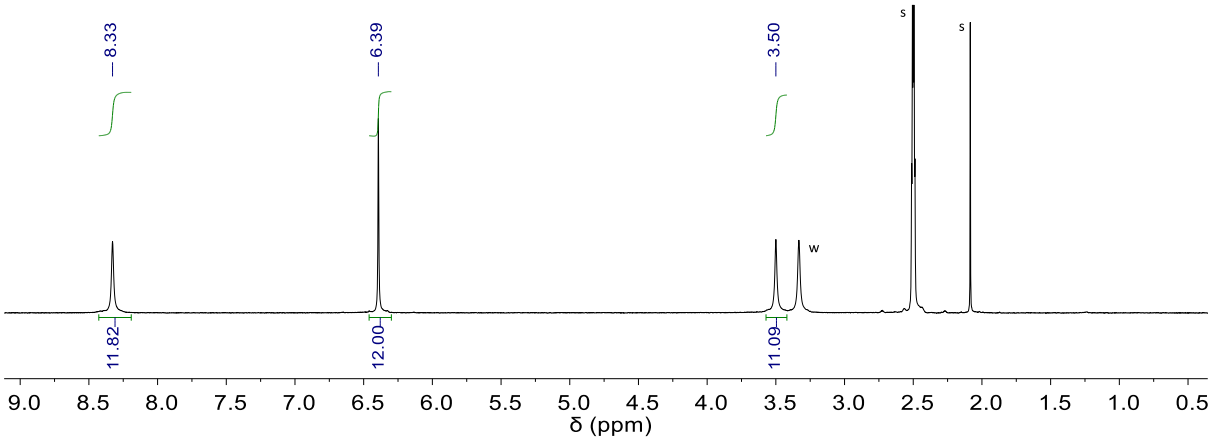

Figure S13. ^{1}H NMR spectrum (300 MHz, DMSO-d_6, 298 K) of **P[6]OH** obtained from **P[6]OMe**. s: solvents, w: water.

2.5. Dodecahydroxypillar[6]arene **P[6]OH** from isolated **P[6]OEt**

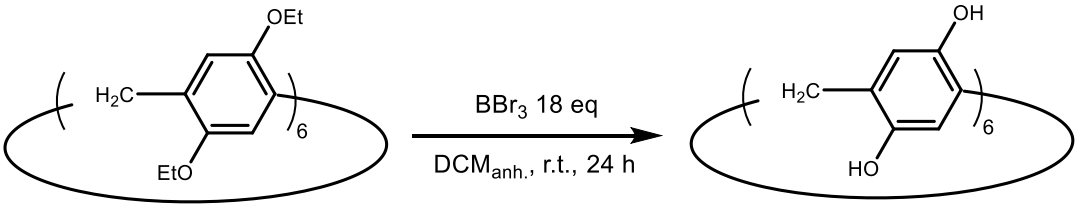

MW: 1069.39
P[6]OEt

MW: 732.74
P[6]OH

In an oven-dried tube equipped with a screw cap, to a stirred suspension of **P[6]OEt** (2.00 g, 1.87 mmol) in anhydrous dichloromethane (94 mL) was added boron tribromide (3.2 mL, d = 2.65 g/mL, 8.48 g, 33.8 mmol, 18 eq.). The mixture was stirred at r.t. (20 °C) for 24h under argon atmosphere. Distilled H_2O (19 mL) was added slowly under vigorous stirring. After 20 min. the precipitate was collected by filtration and washed with distilled H_2O (60 mL) to afford a dark grey solid (1.61 g). The solid was taken up in acetone (100 mL) and the mixture was stirred at 60 °C for 1h30. Upon cooling to r.t., the suspension was filtered and washed with acetone to remove insolubles. The filtrate was evaporated under reduced pressure. The green residue was dissolved again in acetone (120 mL) and cyclohexane was added (240 mL) while stirring at r.t.. The precipitate was collected by filtration and washed with cyclohexane to isolate a light green solid (1.19 g, 1.62 mmol, 86% yield). Spectral data are in accordance with the literature.[S3]

Note: Filtration after quenching the reaction with water afforded **P[6]OH** in quantitative yield, with high purity according to ^{1}H NMR characterization in DMSO-d_6. However, we noticed that this product contained impurities insoluble in acetone that were thus removed by filtration, followed by precipitation with cyclohexane to isolate **P[6]OH** in higher purity. To the best of our knowledge, literature procedures indicate no such purification of **P[6]OH** and purity of crude **P[6]OH** was not investigated in previous reports.

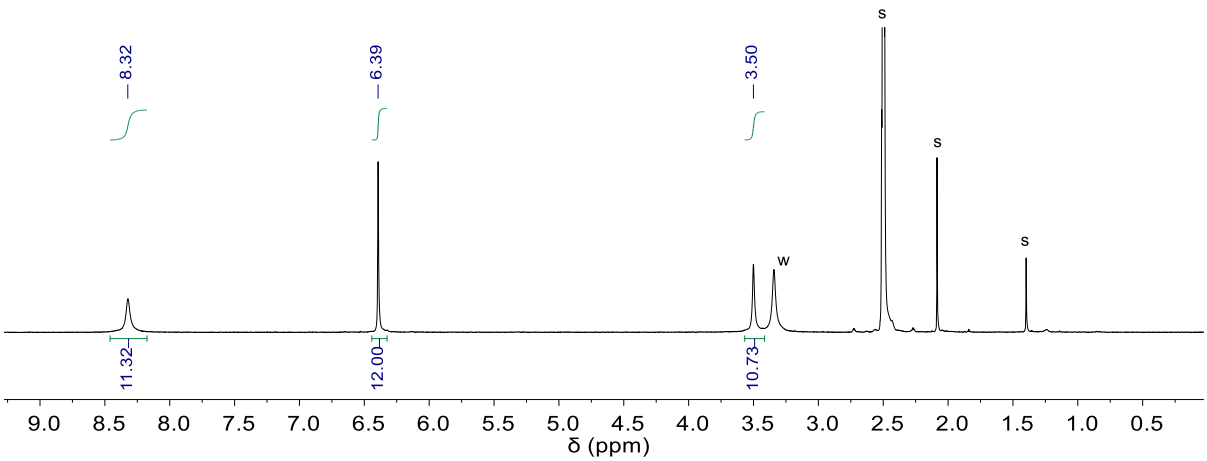

Figure S14. ^{1}H NMR spectrum (300 MHz, DMSO-d_6, 298 K) of **P[6]OH** obtained from **P[6]OEt**. s: solvents, w: water.

2.6. Butylpillar[6]arene **P[6]OBu**

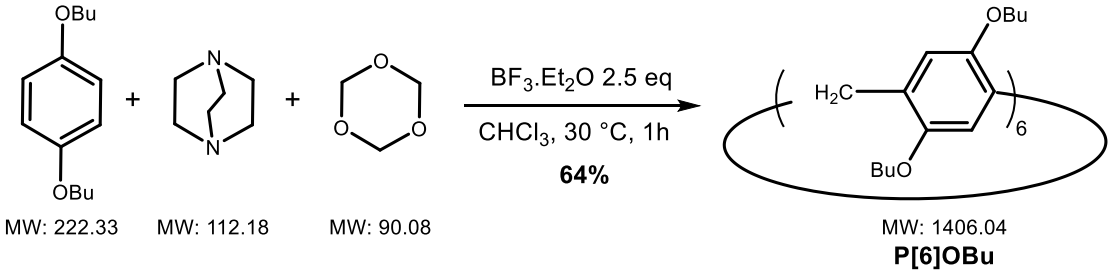

MW: 222.33 MW: 112.18 MW: 90.08 MW: 1406.04

P[6]OBu

In a round bottomed flask, to a mixture of 1,4-dibutylbenzene (1.00 g, 4.50 mmol) and 1,3,5-trioxane (0.276 g, 3.06 mmol, 0.68 eq.) and 1,4-diazabicyclo[2.2.2]octane (0.124 g, 1.11 mmol, 0.25 eq.) in chloroform (22 mL) was added $BF_3{\cdot}Et_2O$ (1.45 mL, d = 1.15 g/L, 1.67 g, 11.8 mmol, 2.62 eq.) while stirring at r.t.. The mixture was then stirred at 30 °C for 60 min. and the color evolved from white to green (after 30 min.) to blue to black (Fig. S15). Quickly after the mixture turned black, the reaction was quenched with methanol (1/4 V = 5.5 mL). The resulting light brown suspension was stirred at r.t. for 24h.

The mixture was filtered and washed with dichloromethane (5 mL). The filtrate was washed with HCl 1 M (30 mL) twice and H_2O (30 mL) twice. The organic layer was evaporated under reduced pressure to afford a brown residue (1.21 g).

The product was purified by flash column chromatography on silica gel (eluent: dichloromethane/cyclohexane 3:2) affording **P[6]OBu** (675 mg, 0.480 mmol, yield: 64%) as a yellow solid. Spectral data is in accordance with the literature.[S1,S4]

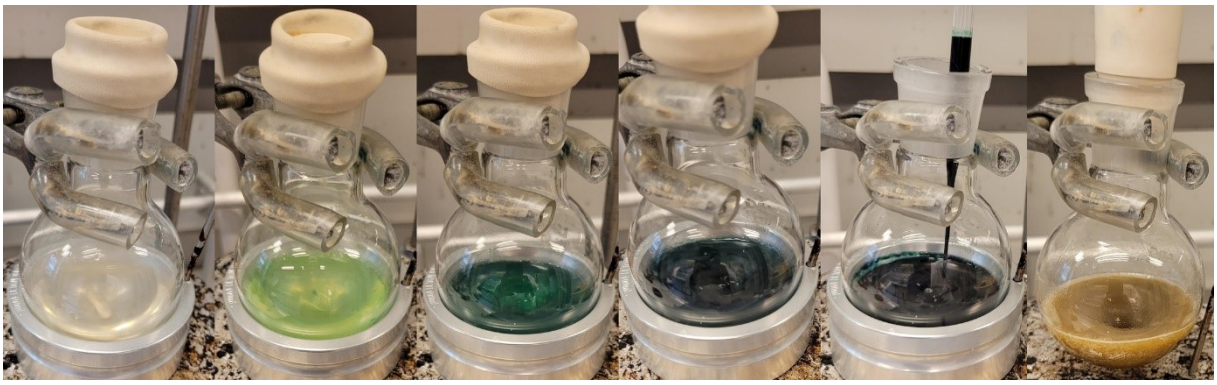

Figure S15. Color evolution of the reaction for the 1 g scale synthesis of **P[6]OBu** in $CHCl_3$, 30 °C (0 min., 25 min., 48 min., 53 min., 57 min., quenching with MeOH).

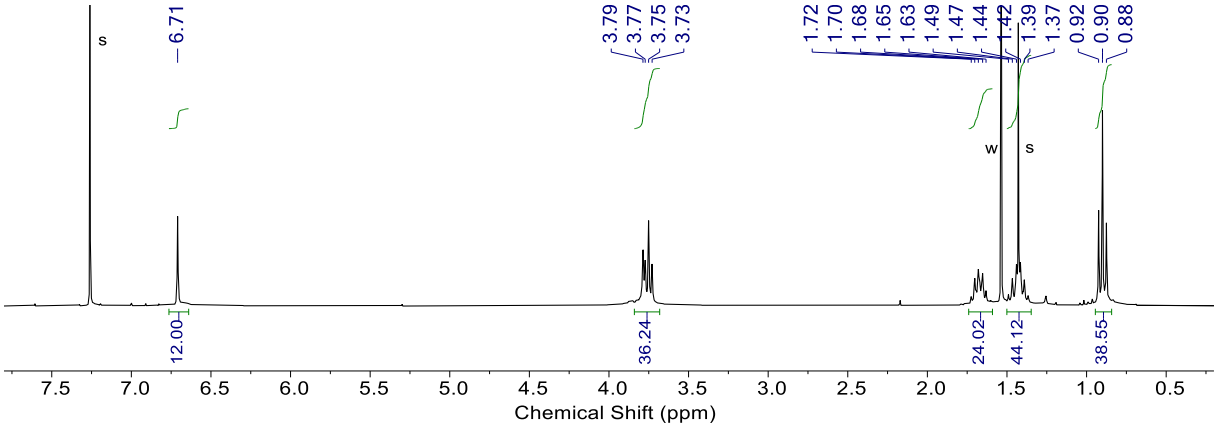

Figure S16. ^{1}H NMR spectrum (300 MHz, $CDCl_3$, 298 K) of **P[6]OBu**. s: solvents, w: water.

3. Reaction monitoring

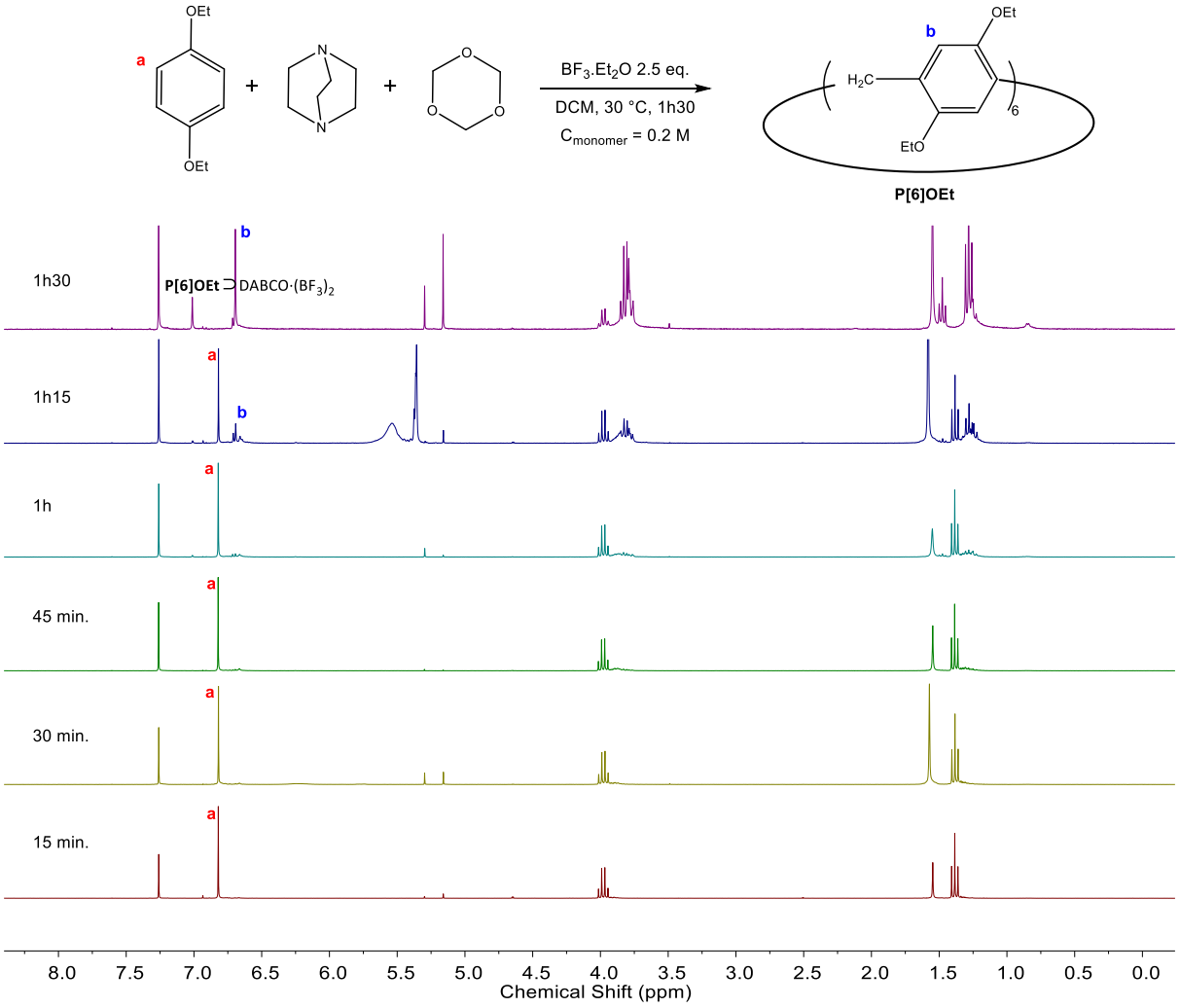

Figure S17. Reaction monitoring for the synthesis of **P[6]OEt** in DCM, 30 °C. Samples were quenched by addition of MeOH, stirred 3h, filtered to remove insoluble polymers, and the filtrate was dried under vacuum.

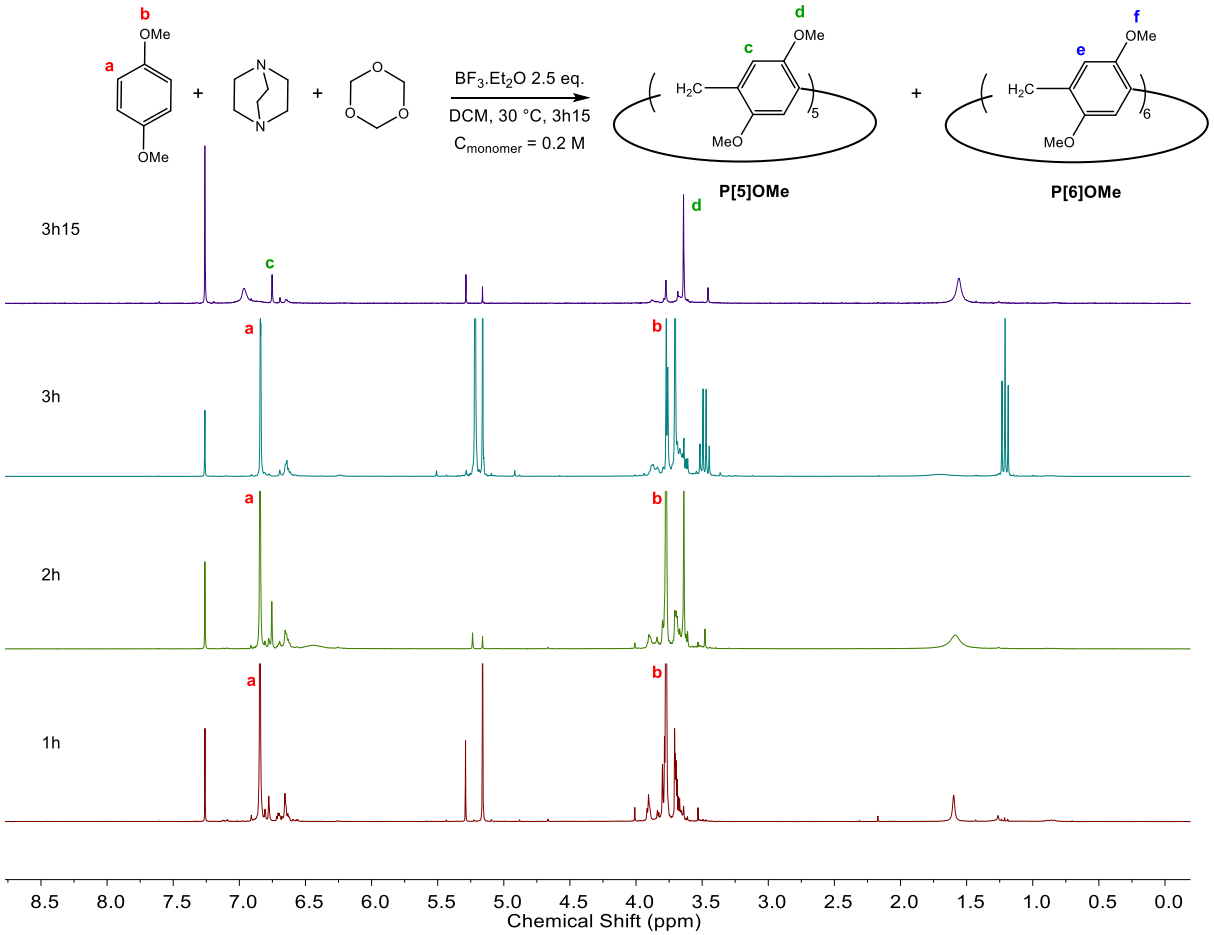

Figure S18. Reaction monitoring for the synthesis of **P[6]OMe** in DCM, 30 °C. Samples were quenched by addition of MeOH, stirred 3h, filtered to remove insoluble polymers, and the filtrate was dried under vacuum.

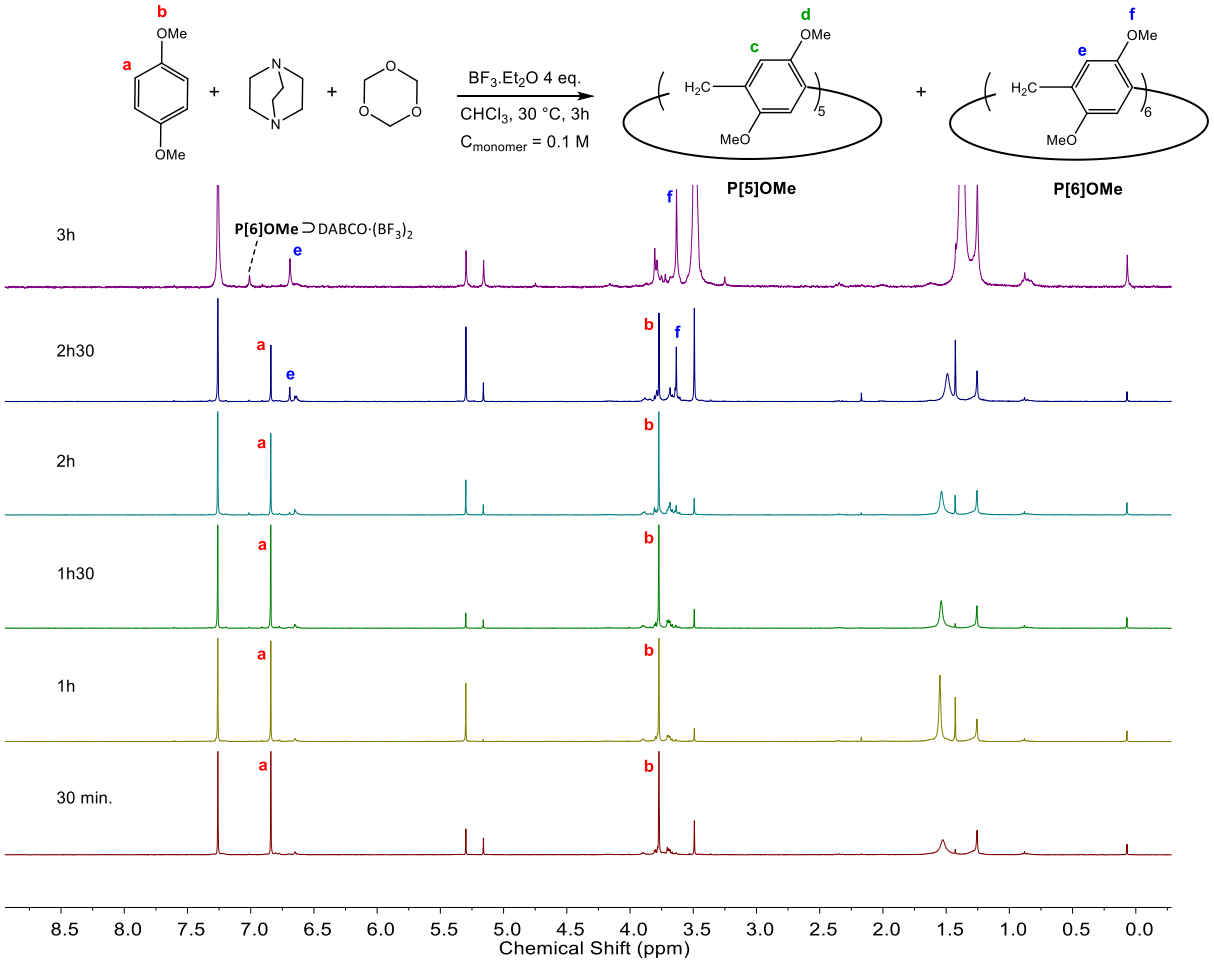

Figure S19. Reaction monitoring for the synthesis of **P[6]OMe** in $CHCl_3$, 30 °C. Samples were quenched by addition of MeOH, stirred 3h, filtered to remove insoluble polymers, and the filtrate was dried under vacuum.

4. Condition screening for pillar[6]arenes synthesis

In addition to the discussion regarding condition screening for **P[6]OEt** templated synthesis in the main text, an extended discussion is provided below with useful but not critical information about some synthesis parameters along Tables S1 (for Lewis acid $BF_3{\cdot}Et_2O$ catalyst) and S2 (for Brønsted acids $MeSO_3H$ and CF_3COOH catalysts).

Tertiary ammonium and Lewis adduct template candidates were prepared *in situ* from the free-base amines and acids (*i.e.* $MeSO_3H$, CF_3COOH, and $BF_3{\cdot}Et_2O$ used as catalyst for the tandem Freidel-Crafts alkylation. Intriguingly, we noticed that significantly more acid quantities than necessary to match the amine equivalents were necessary for the Friedel-Crafts alkylation to start. Initial expectations were 2 or 1 equiv. of acid respective to DABCO or quinuclidine to generate the template + 1 equiv. per substrate **1** to promote the Friedel Crafts alkylation. For screening reactions, acid quantities were thus adjusted by sequential additions of acids until the reaction started, as indicated by a green coloration and thin layer chromatography (TLC) monitoring.

The theoretical minimum amount of template required to fit inside all hexamers potentially formed in the reaction is 0.167 equiv. (*i.e.* $1/6^{th}$). Screening reactions were thus always performed with >0.167 equiv. of template.

We first explored the effect of **DABCO·2BF₃** in chloroform, a solvent with no reported template effect for any pillar[*n*]arene size. Reactions were first performed at low concentration (*i.e.* [**1**] = 0.05 M) to minimize the formation of undesirable polymers. Initial experiments were performed in $CHCl_3$ neutralized on basic alumina to remove traces of HCl, which was reported to play an inhibitor role in this reaction.[S5] No significant changes in the outcome of reactions involving DABCO were observed using $CHCl_3$ directly from bottles of different ages containing traces of HCl. We infer that the use of basic DABCO completely suppresses the effects of trace HCl. Thus, neutralizing the solvent appears unnecessary.

Compared to standard **P[n]OEt** synthesis with $BF_3{\cdot}Et_2O$, where the Friedel-Crafts alkylation starts within seconds as indicated by a green coloration, a striking difference when using DABCO is the significant delay (>40 min. for [**1**] = 0.05 M) in the appearance of green color, likely caused by the initial precipitation of **DABCO·nBF₃** species trapping excess BF_3 and slowly solubilizing throughout the reaction.

The initial low concentration (*i.e.* [**1**] = 0.05 M) used to evaluate template efficiency in the synthesis of **P[6]OEt** led to high yielding conditions with **DABCO·2BF₃** templates (see Table 1 in main text). However, these low concentration methods are impractical for large-scale synthesis due to the large amount of solvent and $BF_3{\cdot}Et_2O$ required, resulting in poor atom economy and cost efficiency (*i.e.* 120 mL of solvent and 3–8 mL of $BF_3{\cdot}Et_2O$ per gram of **1**). We thus explored the concentration effect ([**1**] = 0.1 and 0.2 M) in $CHCl_3$ and CH_2Cl_2 (Table S1). Under these concentrated conditions, smaller amounts of DABCO (0.25 equiv.) and $BF_3{\cdot}Et_2O$ (3 equiv.) were necessary to maintain a high selectivity for the desired hexamer **P[6]OEt** over other oligomers and medium to high yields (44–61%). Indeed, the effective concentration of template precursor DABCO is the same between [**1**] = 0.05 M with 1 equiv. of DABCO, and [**1**]

= 0.2 M with 0.25 equiv. of DABCO. Accordingly, further optimization was performed at this elevated concentration [**1**] = 0.2 M.

Table S1. Screening of concentrations for the synthesis of **P[6]OEt** templated by Lewis adducts.[a]

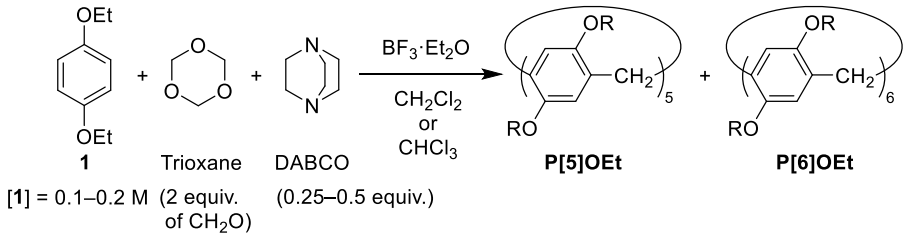

Entry	[1] (M)	Equiv. DABCO	Equiv. $BF_3{\cdot}Et_2O$[b]	Solvent	Yield P[5]OEt	Yield P[6]OEt[c]
1	0.1	0.25	5.0	$CHCl_3$	–[d]	61%
2	0.1	0.5	10	$CHCl_3$	–[d]	54%
3	0.2	0.25	5.0	$CHCl_3$	–[d]	49%
4	0.2	0.5	7.5	$CHCl_3$	–[d]	54%
5	0.2	0.25	3.0	CH_2Cl_2	–[d]	44%
6	0.2	0.5	5.0	CH_2Cl_2	–[d]	53%

[a] All reactants were stirred at r.t. until complete consumption of **1** (2–3h). Scale: 50–100 mg of **1**. After consumption of **1**, products were precipitated by addition of 3V of MeOH and collected by filtration. Solids were stirred in CH_2Cl_2/MeOH, 4:1, at r.t. overnight to degrade Lewis adduct templates. Insolubles were removed by filtration, and the filtrate was dried then filtered through silica gel with (CH_2Cl_2/acetone, 99:1). [b] Quantities of $BF_3{\cdot}Et_2O$ are not always consistent as they were adjusted throughout this preliminary study to ensure reaction start. [c] Isolated yields correspond to a minimum. Fractions of **P[6]OEt** may have been lost in the filtrate of the first filtration. [d] No **P[5]OEt** was observed but traces could have been lost in the filtrate of the first filtration.

Table S2. Screening conditions for the synthesis of **P[6]OEt** templated by ammoniums generated by Brønsted acids.[a]

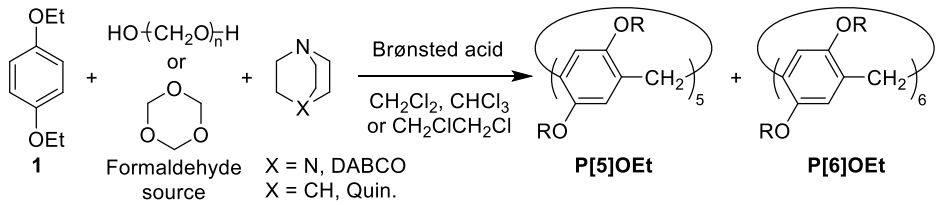

Entry	[1] (M)	Source of formaldehyde (equiv. CH_2O)	Template precursor (equiv.)	Acid (equiv.)[b]	Solvent, T, time	Yield P[5]OEt[c]	Yield P[6]OEt[c]
1	0.05	paraformaldehyde (2)	–	$MeSO_3H$ (3.0)	$CHCl_3$, r.t., 3h30	traces	traces
2	0.05	paraformaldehyde (2)	DABCO (1.0)	$MeSO_3H$ (8.0)	$CHCl_3$, r.t., 3h30	<10%[d]	<16%[d]
3	0.05	paraformaldehyde (2)	Quin. (1.0)	$MeSO_3H$ (7.0)	$CHCl_3$, r.t., 3h30	<5%[d]	<13%[d]
4	0.05	paraformaldehyde (1.5)	DABCO (1.0)	CF_3COOH (15)	$CHCl_3$, 70 °C, 4h	3%	27%
5	0.05	paraformaldehyde (1.5)	DABCO (1.0)	CF_3COOH (15)	CH_2Cl_2, 50 °C, 4h	16%	48%
6	0.05	paraformaldehyde (1.5)	DABCO (1.0)	CF_3COOH (15)	$(CH_2Cl)_2$, 70 °C, 4h	47%	20%
7	0.05	trioxane (2)	DABCO (1.0)	CF_3COOH (48)	CH_2Cl_2, 40 °C, 27h	~15%	~10%
8	0.1	trioxane (2)	DABCO (1.0)	CF_3COOH (32)	CH_2Cl_2, 40 °C, 29h	~9%	~12%
9	0.2	trioxane (2)	DABCO (1.0)	CF_3COOH (20)	CH_2Cl_2, 40 °C, 29h	traces	~6%
10	0.05	paraformaldehyde (2)	DABCO (1.0)	CF_3COOH (16)	CH_2Cl_2, 40 °C, 3h	~14%	~54%
11	0.1	paraformaldehyde (2)	DABCO (1.0)	CF_3COOH (16)	CH_2Cl_2, 40 °C, 3h	~6%	~7%
12	0.2	paraformaldehyde (2)	DABCO (1.0)	CF_3COOH (12)	CH_2Cl_2, 40 °C, 3h	~12%	~31%

[a] Reactions under stirring and under pressure when heated beyond solvent boiling point. Scale: 25–100 mg of **1**. Reactions with $MeSO_3H$ were quenched by addition of MeOH and Na_2CO_3. Reactions with CF_3COOH were quenched by aqueous wash of the organic layer to extract acids. Volatiles were evaporated and crude products were analyzed by ^1H NMR spectroscopy in $CDCl_3$. [b] Quantities of acid were adjusted by gradual additions throughout this preliminary study to ensure reaction start. [c] Yields were calculated by ^1H NMR integration of ArH signals after deconvolution. [d] Yield capped due to large amounts of insoluble polymer byproducts; Percentages correspond to NMR signal ratio in the ArH region for the soluble fraction of crude product.

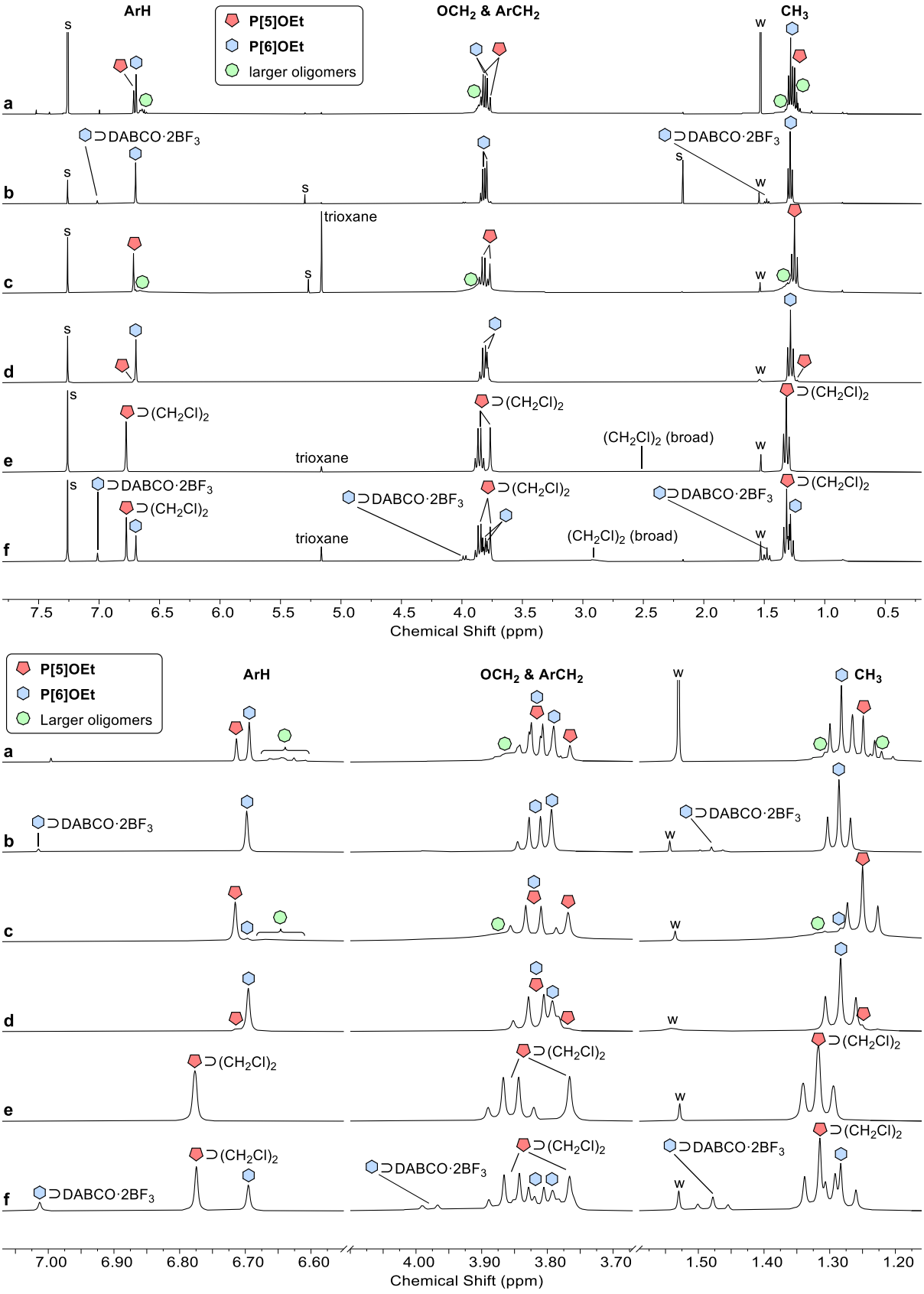

Figure S20. ^{1}H NMR spectra (300 MHz, $CDCl_3$, 298 K) of screening reactions for the synthesis of **P[6]OEt** after filtration in silica gel. Top: full spectra, bottom: selected regions of interest. (a–f) correspond to Entries 1–6 of Table 1. Reaction conditions: (a) $CHCl_3$, (b) $CHCl_3$ with DABCO, (c) CH_2Cl_2, (d) CH_2Cl_2 with DABCO, (e) $(CH_2Cl)_2$, (f) $(CH_2Cl)_2$ with DABCO. w: water. **P[5]OEt** can include residual CH_2Cl_2 or $(CH_2Cl)_2$ in fast exchange on the chemical shift timescale, significantly affecting its ^{1}H signals chemical shift (as seen in e and f).

5. Host–guest studies with **P[6]OEt**

5.1. **P[6]OEt** and **DABCO** binding constant

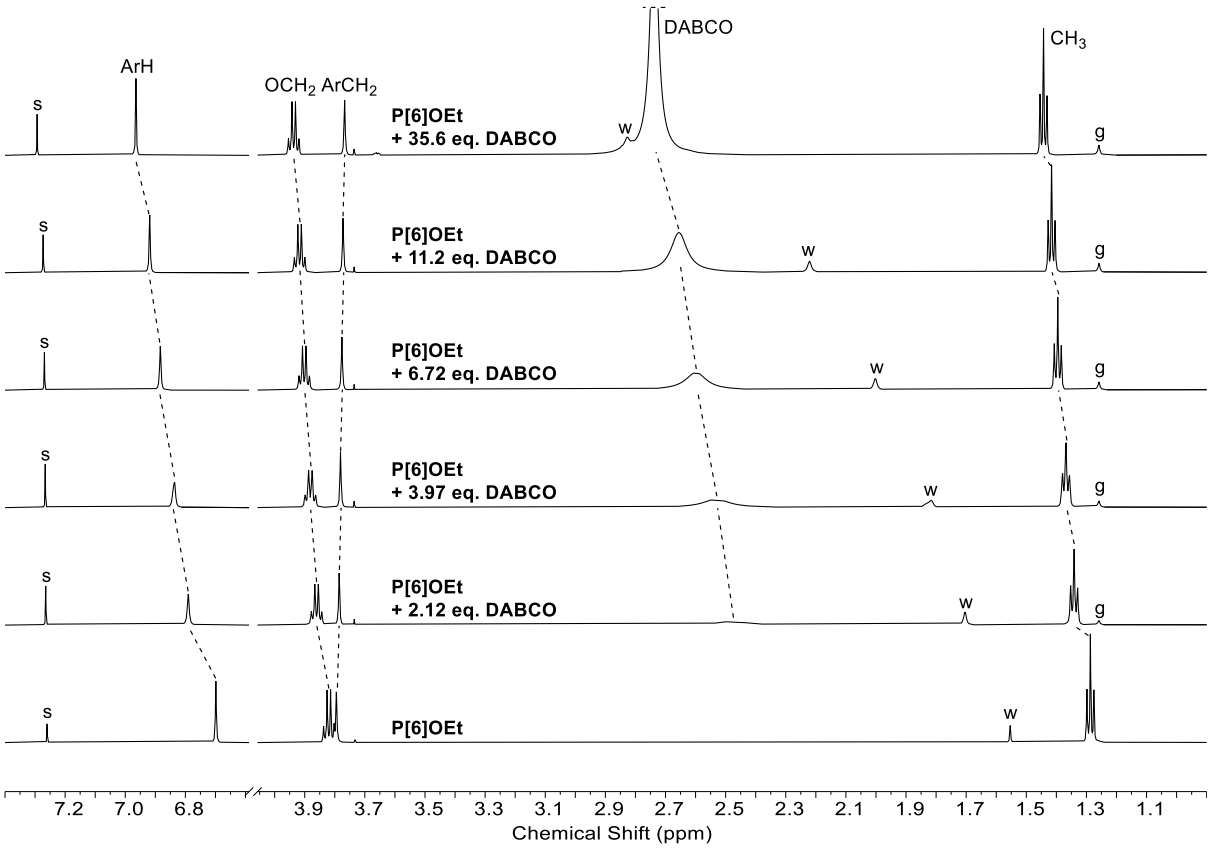

Figure S21. ^{1}H NMR spectra (600 MHz, $CDCl_3$, 298 K) of the titration of DABCO into a **P[6]OEt** (4.5 mM) solution. $CDCl_3$ was passed through basic alumina prior to titration to remove traces DCl. The $CHCl_3$ chemical shift was significantly affected at high concentrations of DABCO, therefore spectra were calibrated on a trace grease signal, which improved signal shifts curve fitting. The complete titration used to determine binding constants contains 11 points (see Figure S22) but only 6 are shown here for clarity. s: solvent, w: water, g: grease.

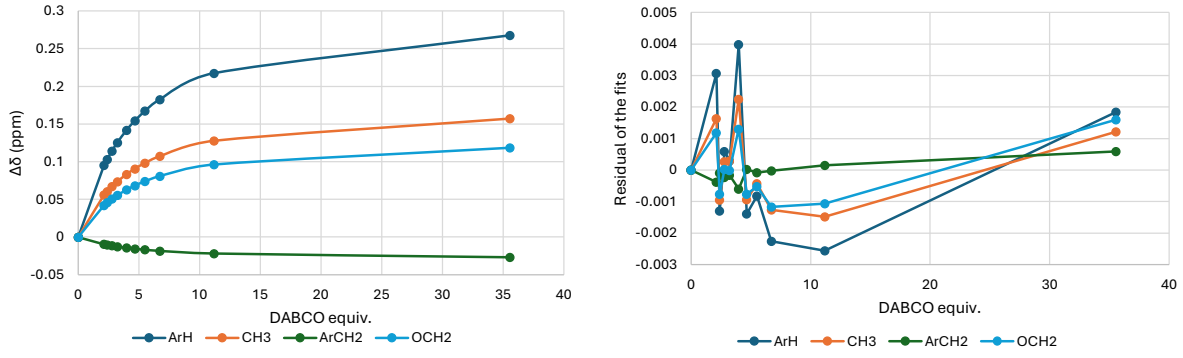

Figure S22. Left: ^{1}H NMR titration data for the formation of **P[6]OEt⊃DABCO** complex (see Figure S21). Right: residual of the curve fitting from BindFit[S6,S7] that determined a binding constant of 58±1 M^{-1} ($CDCl_3$, 298 K).

5.2. **P[6]OEt** and **DABCO-R_2^{2+}** binding

DABCO-R_2^{2+} (R = Me, *n*Pr, *n*$C_{12}H_{25}$) diammonium ions were expected to show higher affinities than **DABCO** for **P[6]OEt**, due to the stronger polarization of C–H bonds. However, the corresponding bromide (for R = *n*Pr, *n*$C_{12}H_{25}$), iodide (for R = Me, *n*$C_{12}H_{25}$), or hexafluorophosphate salts exhibited very poor solubility in apolar chlorinated solvents such as chloroform, even with dodecyl chains. Addition of all these salts at saturation to a solution of **P[6]OEt** in $CDCl_3$ showed negligible shifts of **P[6]OEt** ^{1}H signals (<0.02 ppm). Addition of 10 vol% of CD_3CN or CD_3OD improved the salts solubility but showed no significant improvement in guest recognition, as expected for polar solvents that can stabilize charged species.

This limited affinity of **P[6]OEt** for **DABCO-R_2^{2+}** can be surprising considering that

- Ogoshi and co-workers reported the binding of a **DABCO-R^+** ammonium within the cavity of **P[6]OEt** in $CDCl_3$ with a binding constant of 552±65 M^{-1}.[S8]
- Gaeta and co-workers reported the use of **DABCO-(*n*C_6H_{13})$_2^{2+}$** as a template in chlorinated solvents for prism[5]arenes, another family of oligomeric macrocycles with electron-rich aromatic cavity.[S9]

One explanation to this weak affinity could lie in steric clashes between ethyl groups of **P[6]OEt** and alkyl chains of included **DABCO-R_2^{2+}**, which only occur when alkyl chains are present on both sides of **DABCO** (Figure S23).

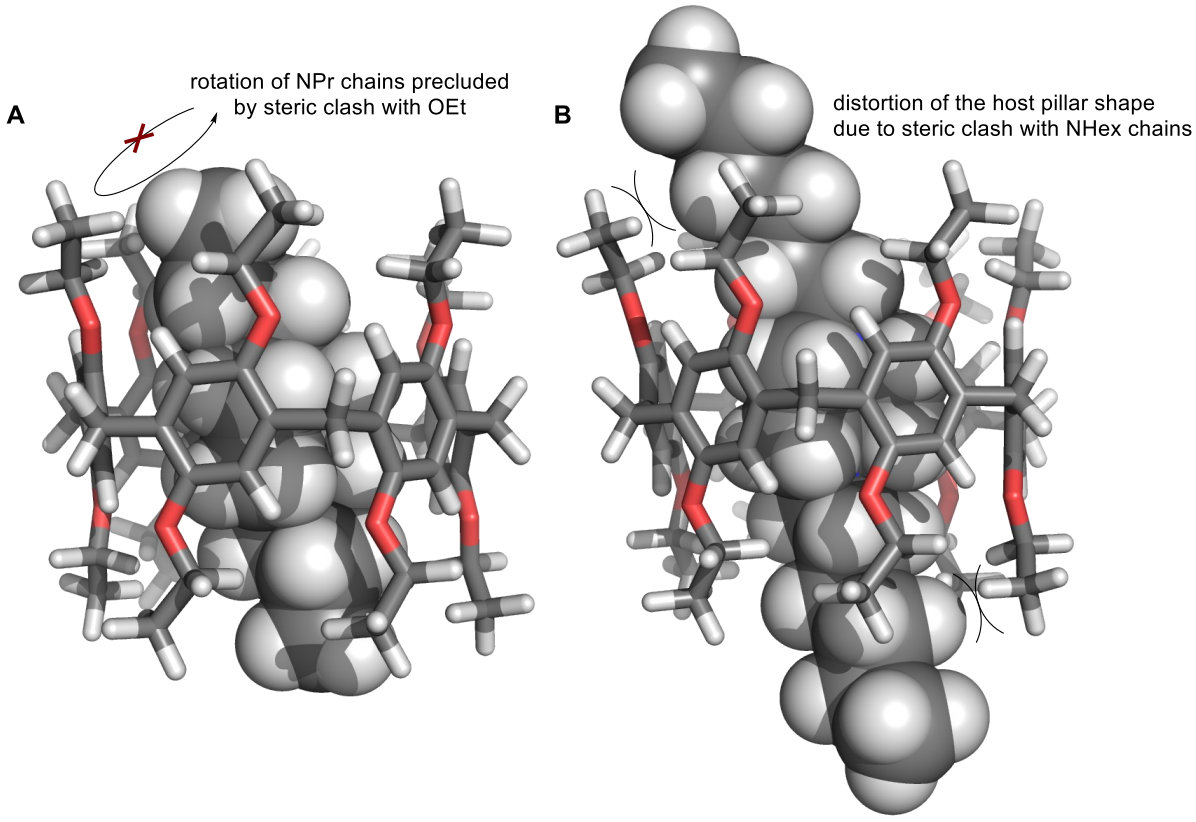

Figure S23. MM2 models of (A) **P[6]OEt⊃DABCO-Pr_2^{2+}** and (B) **P[6]OEt⊃DABCO-Hex_2^{2+}** showing that DABCO-R_2^{2+} guests with alkyl chains longer than ethyl may cause steric clashes with the pillararene host and have restricted conformational freedom.

5.3. **P[6]OEt⊃DABCO·nBF$_3$** inclusion complexes formation and properties

The generation of **P[6]OEt⊃DABCO·2BF$_3$** inclusion complex was attempted by addition of $BF_3{\cdot}Et_2O$ to a mixture of **P[6]OEt** and 1 equiv. of DABCO. However, the weak binding between these species causes most of DABCO to be free in solution. Since DABCO precipitates upon addition of >1 equiv. of $BF_3{\cdot}Et_2O$, most of free DABCO precipitates in the form of **DABCO·nBF$_3$** precluding clean formation of **P[6]OEt⊃DABCO·2BF$_3$** (Figure S24). Nonetheless, two new sets of ^{1}H NMR signals arise in slow exchange with free **P[6]OEt** (Figure S24c). One of these new species exhibits two singlets in the aromatic region at 7.00 and 7.02 ppm which was assigned to the inclusion complex **P[6]OEt⊃DABCO·BF$_3$** where Ar*H* of **P[6]OEt** pointing toward the $N{\cdot}BF_3$, and Ar*H* pointing toward the free amine are differentiated, effectively leading to an apparent C_6 symmetry. The other species exhibits one singlet at 7.01 ppm which was assigned to the **P[6]OEt⊃DABCO·2BF$_3$** complex with an apparent D_6 symmetry. Similarly to DABCO inclusion complex, ArH, OCH_2, and CH_3 signals for these inclusion complexes are downfield shifted compared to free **P[6]OEt**, whereas $ArCH_2$ signals are upfield shifted. An intricate multiplet appears in the high field region at 0.84 ppm (more intense and evident in complementary studies below, Figures S25 and S26), which was assigned to included **DABCO·2BF$_3$** that is significantly upfield shifted compared to typical C*H*$_2$N signals. The exact complexation induced shift is not measurable considering the insolubility of free **DABCO·2BF$_3$** but, for reference, the C*H*$_2$N·BF$_3$ signal of *n*$Bu_3N{\cdot}BF_3$ was measured at 2.81 ppm. The intricate multiplicity is consistent with the enantiotopic hydrogen atoms of **DABCO·2BF$_3$** experiencing the chiral environment inside the cavity of a pillararene.

To circumvent the precipitation of **DABCO·nBF$_3$**, we attempted the generation of **P[6]OEt⊃DABCO·2BF$_3$** in presence of excess DABCO (10 equiv.) by gradual additions of $BF_3{\cdot}Et_2O$ (Figure S25). In this case, **P[6]OEt⊃DABCO·2BF$_3$** is formed as the major species with a maximum amount after addition of 3–4 equiv. of $BF_3{\cdot}Et_2O$ (Figure S25e,f) but coexisting with what appears to be **P[6]OEt⊃DABCO·nH$^+$**, likely protonated by small amounts of HF or HBF_4 from the hydrolysis of BF_3. Further additions of BF_3 cause excessive precipitation and a decrease of **P[6]OEt⊃DABCO·2BF$_3$** amounts (Figure S25g). This Lewis adduct inclusion complex degrades over time in such conditions, likely due to the presence of excess DABCO that may promote the BF_3 cleavage/exchange and, ultimately, degradation or precipitation (Figure S25h).

Interestingly, **P[6]OEt⊃DABCO·2BF$_3$** could be isolated at the end of the **DABCO·2BF$_3$** templated synthesis of **P[6]OEt** by rapid precipitation with excess MeOH. Insoluble polymeric side products are also present in the solid but **P[6]OEt⊃DABCO·2BF$_3$** can be extracted from the solid with CH_2Cl_2 along small quantities of **P[6]OEt⊃DABCO·BF$_3$** and **P[6]OEt**. The properties of these inclusion complexes could thus be more conveniently studied from these samples, compared to aforementioned preparation attempts containing large amounts of side products.

^{1}H NMR analysis of this crude **P[6]OEt⊃DABCO·2BF$_3$** sample (Figure S26) allows a better visualization of the intricate multiplet in the high field region (0.84 ppm), integrating for 12 protons (13 with the overlapping grease signal) that was assigned to included **DABCO·2BF$_3$**, in

accordance with the shielding effect of a polyaromatic cavity and the chiral environment of **P[6]OEt** differentiating enantiotopic ^{1}H of **DABCO·2BF₃**. ^{19}F NMR analysis revealed ^{19}F resonances in the B–F region (between −153 and −164 ppm, see Figure S27).

Addition of small amounts of CD_3OD to the NMR sample readily degraded the binary Lewis adduct **DABCO·BF₃** affording the **P[6]OEt⊃DABCO** inclusion complex in fast exchange with free **P[6]OEt** on the chemical shift time scale (Figure S28b). Degradation of the ternary Lewis adduct, however, required an extended time in presence of protic solvents (e.g. overnight stirring with 10–20v% of MeOH, Figure S28c). Filtration of **P[6]OEt⊃DABCO** through silica gel (CH_2Cl_2/acetone, 99:1) afforded a pure sample of **P[6]OEt** (Figure S28d). We note that traces of **P[6]OEt⊃DABCO·2BF₃** and **P[6]OEt⊃DABCO·BF₃** were occasionally observed in our previous screening reactions, which indicates that these complexes can withstand filtration through silica gel to some extend if Lewis adducts are not thoroughly degraded beforehand.

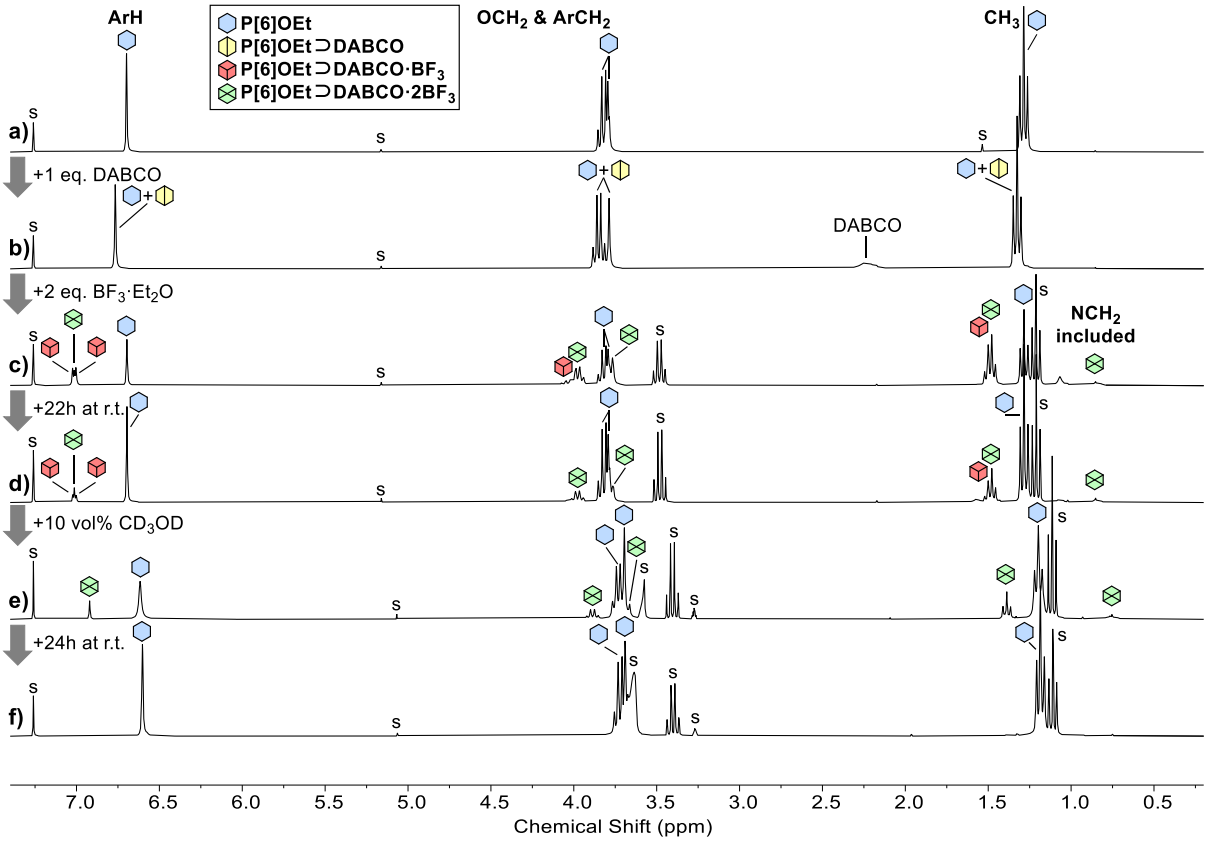

Figure S24. ^{1}H NMR spectra (300 MHz, 298 K, (a–d) $CDCl_3$ or (e–f) $CDCl_3/CD_3OD$, 10:1) of (a) **P[6]OEt** (10 mM), (b) the inclusion complex **P[6]OEt⊃DABCO** in fast exchange with free host and guest, and (c–f) **P[6]OEt⊃DABCO·BF₃** and **P[6]OEt⊃DABCO·2BF₃** in slow exchange with host and guest. (d–f) Evolution over time and after addition of CD_3OD showing a slower degradation of **P[6]OEt⊃DABCO·2BF₃** over **P[6]OEt⊃DABCO·BF₃**. Samples b–f contained **DABCO·nBF₃** precipitate. s: solvents and water.

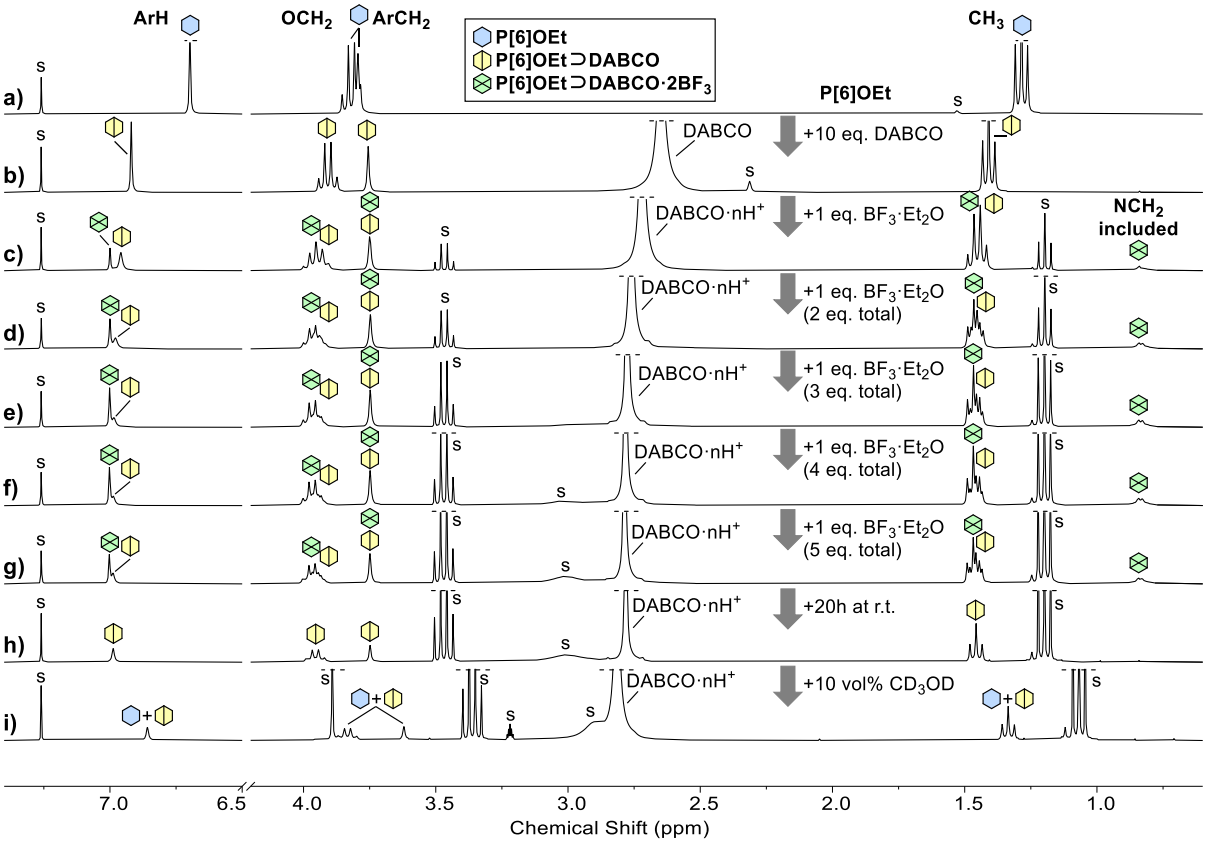

Figure S25. ^{1}H NMR spectra (300 MHz, 298 K, (a–h) $CDCl_3$ or (i) $CDCl_3/CD_3OD$, 10:1) of (a) **P[6]OEt** (10 mM), (b) mostly the inclusion complex **P[6]OEt⊃DABCO** in fast exchange with free host and guest, and (c–g) **P[6]OEt⊃DABCO·2BF₃** in slow exchange with **P[6]OEt⊃DABCO·nH⁺** (like protonated by traces of HF or HBF_4 generated by the hydrolysis of BF_3). (h) Evolution over time showing the slow degradation of **P[6]OEt⊃DABCO·2BF₃**. (i) Evolution after addition of CD_3OD that causes decomplexation of DABCO. Samples e–i contained **DABCO·nBF₃** precipitate. s: solvents and water.

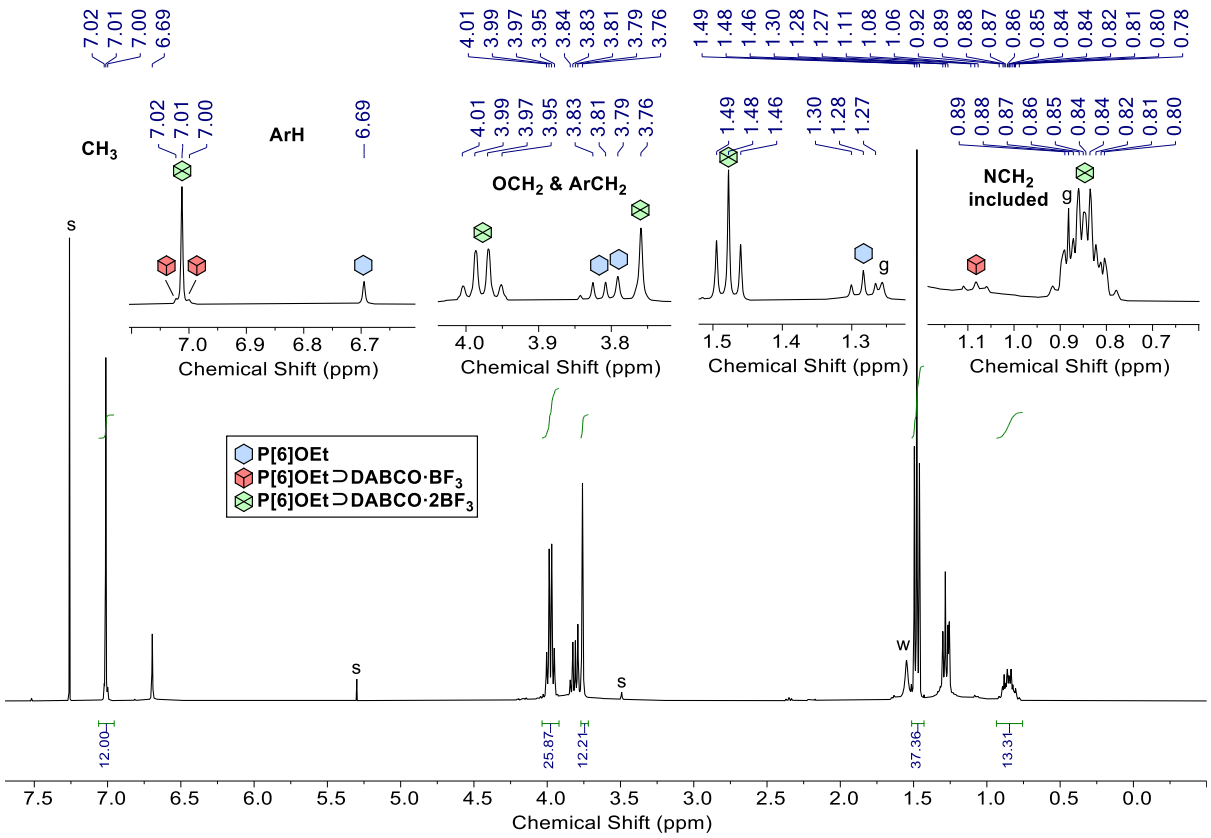

Figure S26. ^{1}H NMR spectrum (400 MHz, $CDCl_3$, 298 K) of **P[6]OEt⊃DABCO·2BF₃** with small amounts of **P[6]OEt⊃DABCO·BF₃** and **P[6]OEt** obtained as crude product of the **DABCO·2BF₃** templated synthesis of **P[6]OEt** by rapid precipitation with excess MeOH.

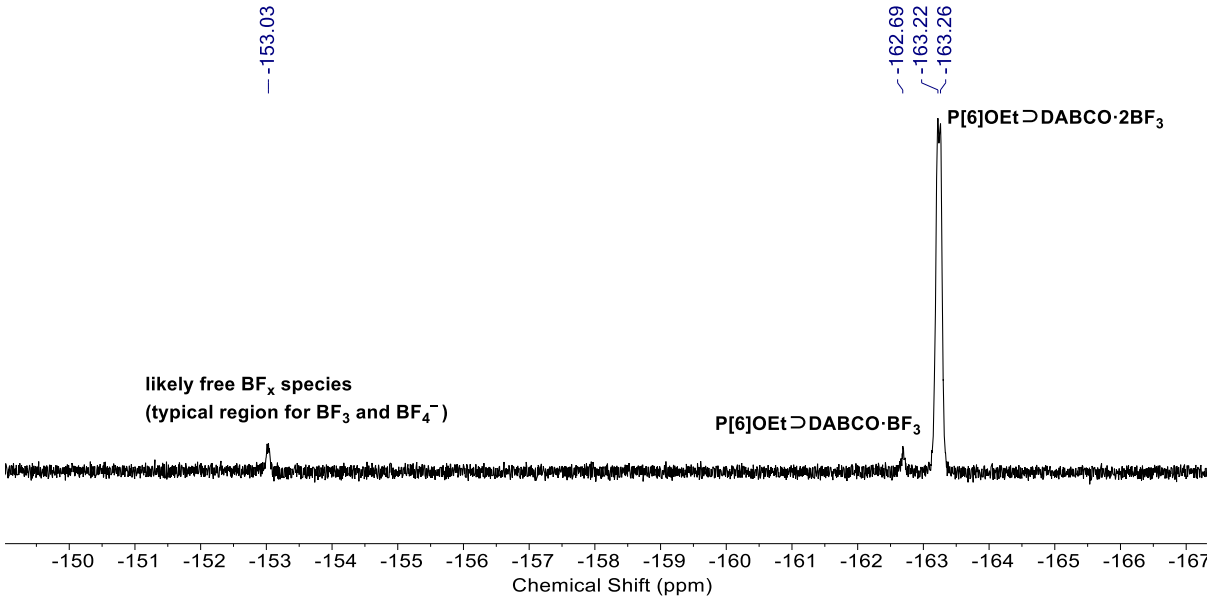

Figure S27. ^{19}F NMR spectrum (376 MHz, $CDCl_3$, 298 K) of **P[6]OEt⊃DABCO·2BF₃** with small amounts of **P[6]OEt⊃DABCO·BF₃** and **P[6]OEt** obtained as crude product of the **DABCO·2BF₃** templated synthesis of **P[6]OEt** by rapid precipitation with excess MeOH.

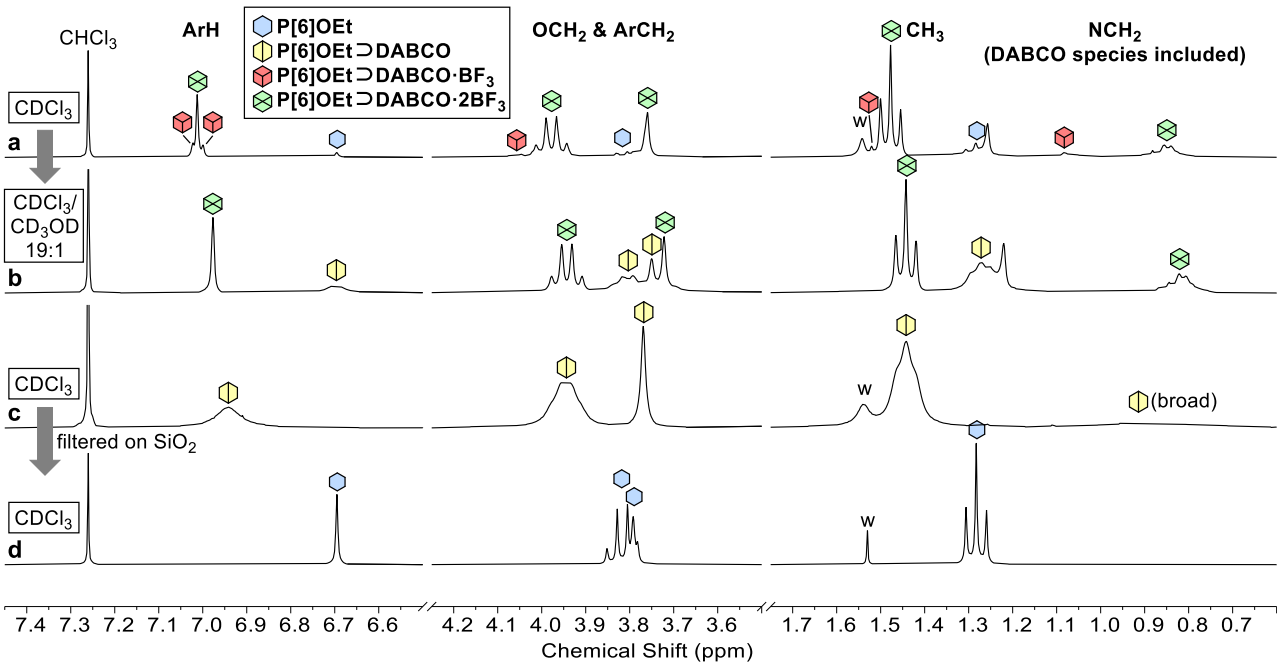

Figure S28. Selected region of ^{1}H NMR spectra (300 MHz, 298 K, (a,c,d) $CDCl_3$ or (b) $CDCl_3/CD_3OD$, 19:1) of products from the **DABCO·2BF₃**-templated synthesis of **P[6]OEt**. (a) Entry 5 of Table S1, $CDCl_3$-soluble fraction of crude product precipitated by addition of excess MeOH, and (b) after addition of CD_3OD, degrading **DABCO·BF₃**. (c) Entry 4 of Table S1, soluble fraction of crude product after stirring in CH_2Cl_2/MeOH (4:1) overnight then dried, degrading **DABCO·nBF₃** (likely acidified to **DABCO·nH^{n+}**), and (d) after further filtration on silica gel (CH_2Cl_2/acetone, 99:1) to remove DABCO. **P[6]OEt** and **P[6]OEt⊃DABCO** are in fast exchange on the chemical shift timescale, whereas **P[6]OEt⊃DABCO·nBF₃** are in slow exchange between them and other species. s: solvents, w: water.

6. Computational studies

Structures for relative energy calculations were optimized by DFT at the ωB97xD/Def2SV(P) level of theory[S10,S11] using the Gaussian 16 program (G16RevC.02) (Gaussian keywords wB97XD/def2SVPP).[S12] The ωB97xD functional was selected because it contains long-range correction to properly model non-covalent interactions. Dichloromethane (ε_r = 8.9) solvent effect was modeled using the Polarizable Continuum Model.[S13] Gibbs Free Energies of reaction (ΔG°) are calculated at 298.15 K and 1 Atm with the Frequency job in Gaussian. No imaginary frequencies were found for optimized structures, ensuring they correspond to a true local or global minimum of the potential energy surface.

6.1. Calculations of pillar[*n*]arene cavity and guest dimensions

The cavity of pillar[*n*]arenes is often described as a cylinder with a diameter of 4.7 Å for the pentamer, and 6.5–6.7 Å for the hexamer. For the present study, cavity diameters were calculated from reported crystal structures as twice the average distance between the center of the cavity and centroids of aromatic rings minus the van der Waals radius of carbon (1.70 Å). Calculated diameters are 4.7 Å for **P[5]OEt** (CCDC 852484), and 6.5 Å for **P[6]OEt** (CCDC 1521814). We note that previous studies reported diameters of 6.6–6.7 Å for pillar[6]arenes.[S14,S15] It may be tempting to evaluate matching guests with their circular diameter, but it can be misleading. Indeed, a simplistic representation of DABCO as a cylinder gives a circular diameter of 6.58 Å (Figure S29), that would barely fit the cavity diameter of 6.5–6.7 Å of pillar[6]arenes. On a closer inspection, the D_{3d}-symmetric structure of DABCO is better described as a ditrigonal prism (*i.e.* a prism with an irregular hexagonal base) with a width of 6.01 Å (Figure S29), which is more suitable to prevent steric clash with the cavity walls.

Other template candidates were considered but exhibit bad size or shape match with the cavity of pillar[6]arenes: Me_4N^+ (6.7 Å in spherical diameter, tetrahedral shape), *t*$BuMe_3N^+$ (6.86 Å in cylindrical diameter, 6.21 Å in hexagonal width), and adamantyltrimethylammonium (7.4 Å in cylindrical diameter).

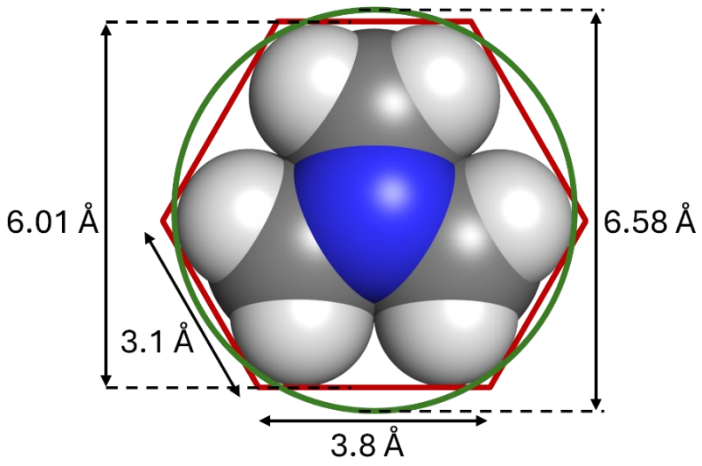

Figure S29. DFT model (ωB97xD/Def2SV(P)) of DABCO viewed along its central C_3 axis with a representation of its circular (green) and ditrigonal (red) dimensions. The circular diameter is calculated as twice the distance of H atoms from the central C_3 axis (2.09 Å) plus the van der Waals radius of hydrogen (1.20 Å).

6.2. Guest binding and conformational stability

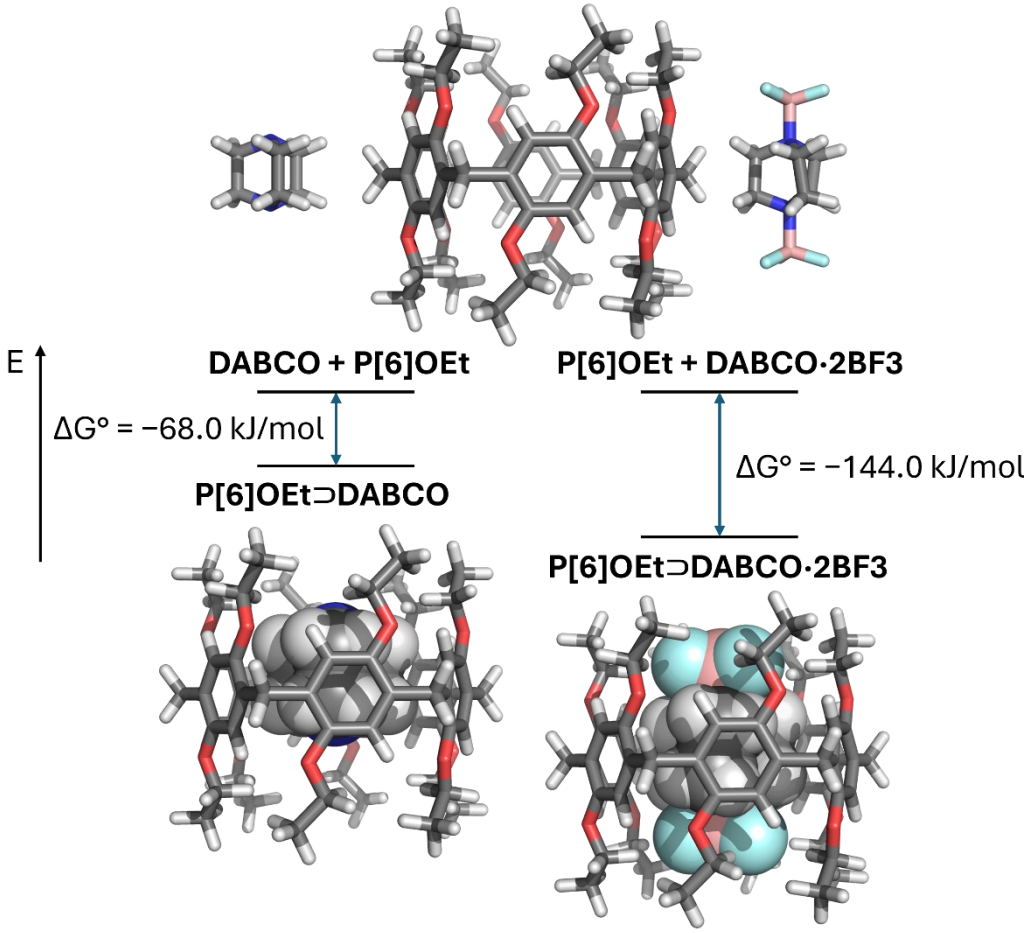

Figure S30. DFT-minimized structures of **P[6]OEt**, **DABCO**, **DABCO·2BF$_3$**, and their inclusion complexes **P[6]OEt⊃DABCO** and **P[6]OEt⊃DABCO·2BF$_3$** at the ωB97xD/Def2SV(P) level of theory in CH_2Cl_2. Note that ΔG° values are likely overestimated compared to real systems in CH_2Cl_2 solutions because solvent molecules may enter the cavity of **P[6]OEt** and partially stabilize it beyond the implicit solvation model used for the calculations.

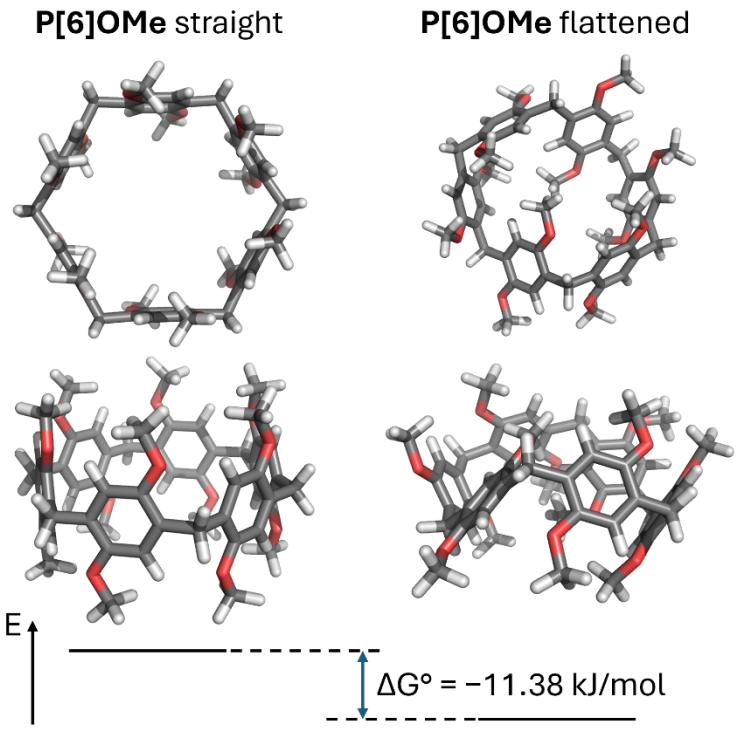

Figure S31. DFT-minimized structures of **P[6]OMe** at the ωB97xD/Def2SV(P) level of theory in CH_2Cl_2 in two local minima: a less stable straight pillar-shape with internal cavity and a more stable flattened shape with no defined cavity. Top: view from the central axis of **P[6]OMe**, bottom: view from the side.

7. References

[S1] S. Mirzaei, D. Wang, S. V. Linderman, C. M. Sem and R. Rathore, *Org. Lett.*, 2018, **20**, 6583–6586, DOI: 10.1021/acs.orglett.8b02937

[S2] M. Da Pian, O. De Lucchi, G. Strukul, F. Fabris and A. Scarso, *RSC Adv.*, 2016, **6**, 48272–48275, DOI: 10.1039/C6RA07164C

[S3] X. Wang, K. Ji, A. Rockenbauer and Y. Liu, Y. Song, *Org. Biomol. Chem.*, 2020, **18**, 2321–2325, DOI: 10.1039/D0OB00341G

[S4] H. Tao, D. Cao, L. Liu, Y. Kou, L. Wang and H. Meier, *Sci. China Chem.*, 2012, **55**, 223–228, DOI: 10.1007/s11426-011-4427-3

[S5] O. Swirepik, J. N. Smith and N. G. White, *J. Org. Chem.*, 2023, **88**, 8310–8315, DOI: 10.1021/acs.joc.3c00305

[S6] P. Thordarson, *Chem. Soc. Rev.*, 2011, **40**, 1305–1323, DOI: 10.1039/C0CS00062K

[S7] D. B. Hibbert and P. Thordarson, *Chem. Commun.*, 2016, **52**, 12792–12805, DOI: 10.1039/C6CC03888C

[S8] T. Ogoshi, H. Kayama, D. Yamafuji, T. Aoki and T.-a. Yamagishi, *Chem. Sci.*, 2012, **3**, 3221–3226, DOI: 10.1039/C2SC20982A

[S9] P. Della Sala, R. Del Regno, C. Talotta, A. Capobianco, N. Hickey, S. Geremia, M. De Rosa, A. Spinella, A. Soriente, P. Neri and C. Gaeta, *J. Am. Chem. Soc.*, 2020, **142**, 1752–1756, DOI: 10.1021/jacs.9b12216

[S10] J.-D. Chai and M. Head-Gordon, *Phys. Chem. Chem. Phys.*, 2008, **10**, 6615–6620, DOI: 10.1039/B810189B

[S11] F. Weigend and R. Ahlrichs, *Phys. Chem. Chem. Phys.*, 2005, **7**, 3297–3305, DOI: 10.1039/B508541A

[S12] M. J. Frisch, G. W. Trucks, H. B. Schlegel, G. E. Scuseria, M. A. Robb, J. R. Cheeseman, G. Scalmani, V. Barone, G. A. Petersson, H. Nakatsuji, X. Li, M. Caricato, A. V. Marenich, J. Bloino, B. G. Janesko, R. Gomperts, B. Mennucci, H. P. Hratchian, J. V. Ortiz, A. F. Izmaylov, J. L. Sonnenberg, D. Williams-Young, F. Ding, F. Lipparini, F. Egidi, J. Goings, B. Peng, A. Petrone, T. Henderson, D. Ranasinghe, V. G. Zakrzewski, J. Gao, N. Rega, G. Zheng, W. Liang, M. Hada, M. Ehara, K. Toyota, R. Fukuda, J. Hasegawa, M. Ishida, T. Nakajima, Y. Honda, O. Kitao, H. Nakai, T. Vreven, K. Throssell, J. A. Montgomery, Jr., J. E. Peralta, F. Ogliaro, M. J. Bearpark, J. J. Heyd, E. N. Brothers, K. N. Kudin, V. N. Staroverov, T. A. Keith, R. Kobayashi, J. Normand, K. Raghavachari, A. P. Rendell, J. C. Burant, S. S. Iyengar, J. Tomasi, M. Cossi, J. M. Millam, M. Klene, C. Adamo, R. Cammi, J. W. Ochterski, R. L. Martin, K. Morokuma, O. Farkas, J. B. Foresman and D. J. Fox, Gaussian 16 (Revision C.02), Gaussian Inc., Wallingford, CT, 2016.

[S13] J. Tomasi, B. Mennucci and R. Cammi, *Chem. Rev.*, 2005, **105**, 2999–3094, DOI: 10.1021/cr9904009

[S14] Y. Ma, X. Chi, X. Yan, J. Liu, Y. Yao, W. Chen, F. Huang and J.-L. Hou, *Org. Lett.*, 2012, **14**, 1532–1535, DOI: 10.1021/ol300263z

[S15] K. Jie, M. Liu, Y. Zhou, M. A. Little, S. Bonakala, S. Y. Chong, A. Stephenson, L. Chen, F. Huang and A. I. Cooper, *J. Am. Chem. Soc.*, 2017, **139**, 2908–2911, DOI: 10.1021/jacs.6b13300